FINAL REPORT

SHARP FLAT PLATE HEAT TRANSFER IN HELIUM AT MACH NUMBERS OF 22.8 TO 86.8 AND IN CORNER FLOW WITH AIR AT MACH NUMBER OF 19

BY H.T. NAGAMATSU AND R.E. SHEER, JR.

Prepared under Contract No. NASW-1785 by

GENERAL ELECTRIC RESEARCH AND DEVELOPMENT CENTER

Schenectady, New York

for NASA Headquarters, Office of Advanced
Research and Technology, Research Division

August 26, 1971

FOREWORD

This report was prepared under contract No. NASW-1785 for NASA Headquarters, Office of Advanced Research and Technology, Research Division, under the technical direction of Messers. I.R. Schwartz and A. Gessow. The research was conducted at the Mechanical Engineering Laboratory, General Electric Research and Development Center in Schenectady, New York.

SUMMARY

Surface heat transfer rates were measured on a sharp flat plate at zero angle of attack with helium over a Mach number range of 22.8 to 86.8 in a hypersonic shock tunnel. The density and leading edge Knudsen number were varied to span the continuum to near free molecule regimes. The strong interaction parameter, $M_1^3/\sqrt{Re_x}$, varied from 11 to 16,000 with Knudsen numbers from 0.56 to 17.1 respectively. For unit Reynolds numbers greater than approximately 15,000 the rate of change of the heat transfer coefficient with $M_1^3/\sqrt{Re_x}$ agreed well with the strong interaction prediction of Li and Nagamatsu. But for lower unit Reynolds numbers there was a systematic reduction in the heat transfer rate close to the leading edge region from the theoretical values.

Local heat transfer rates in the corner flow region produced by the intersection of two perpendicular flat plates with sharp leading edges were determined with air at a Mach number of 19 for various flow densities. The strength of the shock wave from the vertical plate was varied by adjusting the angle of attack from 0 to 5°. The unit Reynolds number varied from 1,000 to 17,200 and the Knudsen numbers from 1.6 to 27. The strong interaction parameter varied from 14 to 500. At low density conditions, with 5° angle of attack for the vertical plate, the local heat transfer rates were increased approximately 70 percent in the vicinity of the corner region, but at continuum flow conditions the heat transfer rates were not increased as much. For the horizontal plate alone in high density flow conditions the heat transfer rates agreed with the strong interaction theory of Li and Nagamatsu. And with the vertical plate the heat transfer rates in the corner region for the horizontal plate were greater than the theoretical prediction.

TABLE OF CONTENTS

LIST OF FIGURES

LIST OF SYMBOLS

C_h	heat transfer coefficient (Stanton number)
C_p	specific heat at constant pressure
C_v	specific heat at constant volume
D	coefficient from Ref. 15
E	voltage
H	enthalpy
I	current
k	thermal conductivity
Kn	Knudsen number
M	Mach number
P	pressure
q	heat transfer rate
R	resistance or gas constant
Re/in	unit Reynolds number
Re_x	length Reynolds number
S'(0)	coefficient from Ref. 40
t	leading edge thickness or time
T	temperature
v	velocity
$\bar{v}$	average molecular velocity
$\bar{V}_\infty$	rarefaction parameter
α	gage resistivity

γ	ratio of specific heats
λ	mean free path
μ	viscosity
ν	kinematic viscosity
ξ	time for one molecular collision
ρ	density
τ	variable of integration
χ	strong interaction parameter

Subscripts

a	conditions after a normal shock
b	gage backing material or conditions before a normal shock
o	initial conditions
f	final conditions
w	wall conditions
w,i	insulated wall conditions
l	leading edge conditions
5	stagnation conditions

1.0 INTRODUCTION

The development of future hypersonic cruise airplanes and space shuttles will require knowledge regarding the hypersonic viscous flow in the immediate vicinity of a leading edge of the lifting surface and in the corner region of the junction between two surfaces. These hypersonic flights will be made at high altitudes where the density is low and for the space shuttle the flight reentry will be at a Mach number of 26 in free molecule flow conditions. As the space shuttle re-enters the earth's atmosphere the free stream conditions ahead of the lifting surface will go from free molecule, to rarefied, and then to continuum flow regimes at lower altitudes and the Mach number will decrease from approximately 26 to subsonic Mach number at landing. There is also a need for information regarding the shock wave and viscous interaction phenomenon for flight Mach numbers greater than 100 for space vehicles entering Jupiter's atmosphere and for re-entering the earth's atmosphere from distant planets.

At these hypersonic flight Mach numbers the flow phenomenon in the corner region between the intersection of the lifting surface with the body and the fin surfaces is very complicated and only limited experimental data has been obtained. Some preliminary results for the space shuttle configuration have indicated large increases in the local heat transfer rates in the region of the shock wave impingement on the lifting surface. For the flight trajectory of hypersonic vehicles the hypersonic viscous flow in the corner region will occur over a range of flow conditions from free molecule to continuum flow regimes depending upon the altitude. For both the lifting surface and the corner region, the local induced pressure, heat transfer rate, and skin friction will depend upon the flight Mach number, altitude, and the configuration of the hypersonic vehicle. At present the available experimental and theoretical references on the rarefied hypersonic flow phenomena are still limited because of the complexity of the flow and the difficulty of obtaining experimental and theoretical results. The applicability of the Navier-Stokes relations has not been established for the low density hypersonic flow conditions.

Sharp flat plates have been used to investigate the shock wave and boundary layer formation in rarefied hypersonic flow conditions in various experimental facilities. With a flat plate the theoretical treatment of the leading edge flow phenomena is simplified because it is two-dimensional over most of the flat plate surface. Even with the sharp flat plate for the experimental study of the viscous effects in the vicinity of the leading edge in the transitional region from continuum to free molecule flows, it is very difficult to obtain the detailed flow structure. The experimental investigations[1-12] have indicated that close to the leading edge of a sharp flat plate the flow can be described approximately on the

basis of kinetic theory. And downstream of this region the shock wave and boundary layer are merged with velocity slip and temperature jump for rarefied hypersonic flow conditions. The length of the non-continuum flow region is dependent upon the free stream Mach number and the leading edge bluntness of the body. Downstream of the region of slip flow at the surface the shock wave and boundary layer are merged with no slip flow at the surface as originally postulated by Shen[13] and Li and Nagamatsu[14,15] as the strong interaction region. Farther downstream the shock wave and boundary layer become separated and a large distance from the leading edge the shock wave becomes weak. Various investigators[16-18] have analyzed the strong interaction region at hypersonic Mach numbers with no slip flow at the plate surface and the results are similar. But when the rarefied flow effects are large, both local induced pressure[2,4,7] and heat transfer rates[3,5,6,12] are much less than that predicted by the strong interaction theories with no wall slip.

Theoretical studies[19-28] have been conducted to solve the flow phenomenon in the vicinity of a sharp flat plate in low density hypersonic flows by assuming a flow model. The existing theories are still inadequate for accurate prediction of the induced pressure, local heat transfer rate, skin friction, and shock wave boundary layer shapes for two- and three-dimensional surfaces at hypersonic rarefied flow conditions encountered in the atmosphere. In the immediate vicinity of the sharp leading edge for low density conditions the flow may be considered as being in the near free molecule region. Nagamatsu and Li[19] applied the kinetic theory concept to show that the slip flow region is a function of the free stream mean free path and the flow Mach number. More recently Bird and colleagues[21-23] have examined the flow near the leading edge of a sharp flat plate and cones by means of a Monte Carlo molecular assumption with the use of digital computational technique. In general the comparison of the overall picture of the flow produced by the theory is in reasonable agreement with the experimental data. The leading edge flow field has been treated by the molecular approach of kinetic theory using the nonlinear Boltzman equation by Huang and Hwang[24], and the agreement with experimental results was approximately correct. A flow model based on an integral approach has been developed by Chow[25] to study the hypersonic rarefied flow over a flat plate. By assuming the shock wave and boundary layer as being merged at the leading edge in low density flows, Shorestein and Probstein[26], Rudman and Rubin[27], and Eiler[28] have obtained solutions with velocity slip and temperature jump at the surface. The analytical predictions of the rarefied hypersonic flow from these theories are still approximate and will require further refinements in the analysis to obtain

better agreement with the observed hypersonic flow phenomena for sharp flat plates.

The three-dimensional hypersonic viscous flow interaction occurring in the corner region of the intersection of two perpendicular surfaces is encountered in the design of high performance hypersonic airplanes and only a limited number of references[29-34] are available on the subject. The corner flow fields influence the local heat transfer and skin friction to the hypersonic vehicle components. Charwat and Redekeopp[29] investigated the corner flow produced by the intersection of two wedge surfaces at a supersonic Mach number range of 2.5 to 4. They observed the shock structure in the corner region which divided the interference field into four distinct zones. Nardo and Cresci[32] determined the local heat transfer rates and induced pressures as well as the shock wave structure along the corner region of two intersecting sharp flat plates in rarefied Mach 11.2 free stream flow. From the impact probe survey in the corner region they observed the complex shock configuration in the viscous region. Stainback and Weinstein[30,31] investigated the corner flow phenomena and local heat transfer distributions at a Mach number of 8. The viscous interaction of the boundary layers in the corner region resulted in a decrease in the local skin friction and heat transfer very near the corner. But a vortex system and reattachment of the boundary layer downstream of the shock-induced separation resulted in an increase in heating outboard of the mutual boundary-layer interaction region. Viscous interactions which arise in regions of high compression on high Mach number vehicles are discussed in Ref. 34. Pal and Rubin[33] have attempted to solve the hypersonic viscous flow in the corner region by the method of asymptotic expansion of the governing equations.

The present paper presents the heat transfer results for the leading edge phenomena on a sharp flat plate in helium flow over a Mach number range of 22.8 to 86.8, where the flow was nearly continuum at the lower Mach numbers and rarefied flow at the higher Mach numbers. In the previous reference 6 the local heat transfer rates were determined at Mach numbers of 67.3 and 86.8 where rarefied flow effects were pronounced and consequently, for the present investigation the lower Mach numbers of 22.8 and 43.3 were selected to produce high density flow conditions in the test section. For these flow Mach numbers in the test section the leading edge Knudsen number varied from 0.56 to 17.1 and the strong interaction parameter ranged from 12 to approximately 13,000. The effects of a monatomic gas compared to the diatomic gases on the rarefied hypersonic flow phenomena were studied by the use of the helium gas instead of air as presented in most published experimental

data[1-12]. The local heat transfer rates for the flat plate at these high Mach numbers are correlated with the strong interaction theory of Li and Nagamatsu[14,15] and the free molecule flow values with the assumption of diffuse reflection at the surface.

The local heat transfer rates in the corner region of two intersecting flat plates with sharp leading edges are presented for the vertical plate at angle of attacks of 0°, 2-1/2° and 5°. Local heat transfer rates were measured on the horizontal plate with air as the test gas at a Mach number of 19. The free stream density conditions were selected to produce continuum to rarefied flow conditions in the test section by varying the reflected stagnation pressure at the entrance to the nozzle while keeping the stagnation temperature and the Mach number in the test section nearly constant.

2.0 EXPERIMENTAL APPARATUS AND INSTRUMENTATION

2.1 Hypersonic Shock Tunnel and Instrumentation

The tests with helium and air in the driven tube of the hypersonic shock tunnel were conducted in the straight through test section of a multiple nozzle, combustion driven shock tunnel described in Ref. 35. For these tests the 4 in. diameter 103 ft. long driven tube was evacuated and filled with helium or dry air as the working gas. The 20 ft. long 6 in. diameter driver was filled with 75 percent helium and stoichiometric mixture of hydrogen and oxygen. There are eighteen tungsten spark plugs to ignite the mixture in the driver to produce the desired shock wave in the driven tube. A reflected type conical nozzle[35,36] with a total angle of 30° and an exit diameter of 24 in. was attached to end of the driven tube. The nozzle is placed inside a 200 cubic foot dump tank which is evacuated to less than 3 microns of mercury to facilitate the flow establishment in the nozzle. A scored diaphragm is placed just upstream of the nozzle entrance which bursts with the arrival of the incident shock wave. The throat diameters for the present investigation to produce helium flow Mach numbers of 22.8, 43.3, 67.3, and 86.8 were 1.0, 0.335, 0.190, and 0.100 in. respectively. For the corner flow investigation with air, the throat diameter of 0.190 in. was used to produce a flow Mach number of 19 in the test section. The incident shock wave reflected from the end of the 4 in. driven tube and the compressed and heated helium and air produced by the reflected shock wave expands into the nozzle to produce the rarefied hypersonic flows in the test section.

A Berkeley counter was used to measure the shock velocity over a 2.5 foot section of the driven tube just ahead of the nozzle entrance. And the reflected stagnation temperature was determined from the measured shock velocity and by assuming the flow to be in equilibrium after the shock waves. The reflected stagnation pressure at the entrance to the nozzle was measured with a Kistler quartz piezoelectric transducer with a response time of approximately 20 microseconds. To minimize the vibrations due to the opening of the scribed diaphragms at the driver and at the end of the driven tube, the flat plate model was mounted on a hollow sting independently supported and isolated from the dump tank and the floor. The shielded electrical leads from the piezoelectric impact pressure and sputtered platinum heat gages were brought out through the sting to the amplifiers before going to the oscilloscope. A detailed description of the shock tunnel and general instrumentation is presented in Refs. 35 and 36.

2.2 Flat Plate Models

The horizontal steel flat plate model, Figs. 1a and 1b, used for the heat transfer investigations with helium and air was 10 inches wide and 16 inches long. With this model it is possible to vary the leading edge thickness from 0.001 to 0.500 in. by attaching thicker pieces at the bottom wedge surface of the plate. The wedge angle for the plate was 15°, and two thin side plates were attached to the horizontal plate with heat gages to prevent the disturbances from the lower surface affecting the heat transfer measurements. At the plane of the leading edge of the flat plate a piezoelectric impact pressure probe was mounted, Fig. 1a, to determine the free stream Mach numbers for helium and air flows in the test section. For the investigation of heat transfer distribution in hypersonic corner flow with air, a flat plate with dimensions of 6 in. and 16 in. with leading edge thickness of 0.001 in. was mounted perpendicular to the horizontal plate as shown in Figs. 1a and 1b. This vertical plate was adjustable relative to the lateral distance from the centerline as well as the angle of attack relative to the free stream as indicated in Fig. 1b. For the present investigation of the hypersonic corner flow phenomena on the local heat transfer distributions, the vertical plate was placed 3/4 in. from the centerline at the leading edge and the angle of attacks of 0, 2-1/2, and 5° were used to produce shock waves of different strengths as indicated in Fig. 1b.

Thirteen sputtered platinum heat gages were located along the center of the horizontal flat plate, Fig. 1a, at the following distances from the leading edge: 0.19, 0.390, 0.580, 0.770, 1.095, 1.405, 2.090, 2.795, 4.04, 5.535, 8.10, 10.55, and 12.945 inches. The heat transfer gages were sputtered platinum[3,6,7] on a backing of Pyrex to a thickness of approximately 350Å and insulated by a thin film of silicone dioxide. Two different sets of sputtered platinum heat gages were used to determine the local heat transfer rate along the plate surface for helium at very high Mach numbers. Another set of heat gages were used in the investigation of the heat transfer distribution in the corner flow region with air. Both heat gages and impact pressure gage were dynamically calibrated in the 8-inch diameter shock tube, before and after each series of tests as discussed in Ref. 37. Both flat plate models were mounted with the horizontal plate on the center of the conical nozzle just downstream of the exit.

3.0 TEST CONDITIONS AND DATA REDUCTION

3.1 Flow Conditions in the Test Section for Helium and Air

The reflected stagnation temperatures at the end of the driven tube for both helium and air were calculated by the shock wave equations and assuming the gas to be in equilibrium for air. Since helium is a noble gas it was assumed to be a perfect gas for the test conditions utilized in the investigation. The temperature and pressure in the driven tube were measured before each shot and the shock velocity was measured at the end of the tube, and these values were used to calculate the reflected stagnation temperature, T_5. With helium the reflected temperature was approximately 2400°R so that the ratio of specific heats was taken to be 1.67 in calculating the flow condition in the conical nozzle. With air the reflected temperature was also approximately 2400°R and consequently the expansion process in the nozzle was assumed to be in thermodynamic equilibrium[38,39].

The reflected pressure and temperature for the helium tests were approximately 1300 psia and 2400°R respectively for the flow Mach numbers in the test section of 22.8, 43.3, 67.3, and 86.8. At the lower Mach numbers the density in the test section was high enough for continuum flow conditions while at the higher Mach numbers the densities were low enough for rarefied flow effects to be present. To investigate the hypersonic corner flow heat transfer with air at a Mach number of 19, the reflected stagnation pressures, P_5, were approximately 80, 300, and 1300 psia with stagnation temperatures of approximately 2400°R. These reflected pressures were selected from the previous investigations, Ref. 5, on the heat transfer rates for a flat plate in continuum to rarefied flow conditions.

3.2 Heat Transfer Gage Data Analysis

The heat gages were mounted in a flat plate and placed in the center of the 8 in. diameter calibrating shock tube[37] to obtain the gage calibration. A piece of plexiglas, which extended 8 in. forward from the leading edge and along the side of the flat plate, was used to produce surface conditions that simulated a wall mounting of the flat plate. The thin platinum film on the backing material of the heat transfer gage is thin enough such that the thermal effects of the platinum can be neglected in comparison to the backing material of pyrex. As a weak shock wave passes over the heat gage, there is a step rise in the temperature of the gage which produces a voltage change across the gage. For a step temperature increase, the heat transfer rate q(t) for the

assumed semi-infinite backing material is given by

$$q(t) = \left(\frac{(\rho C_p k)_b}{\pi}\right)^{1/2} \frac{\Delta T}{\sqrt{t}} = \left(\frac{(\rho C_p k)}{\pi}\right)^{1/2} \frac{\Delta E}{\alpha I R_0 \sqrt{t}} \tag{1}$$

where $(\rho C_p k)_b$ are the density, specific heat, and thermal conductivity respectively of the backing material for the thin film gages, and ΔT is the temperature rise of the gage, which is observed as the voltage change ΔE on the oscilloscope. The change in the gage resistance, ΔR, due to a surface temperature change, $\Delta T \approx T_f - T_0$, is

$$\Delta R = R_f - R_0 = R_0 \alpha \Delta T \tag{2}$$

where R_0 and R_f are the gage resistances at temperatures T_0 and T_f, and α is the resistivity. The heat gage is operated at a constant current I and hence the voltage change ΔE across the gage for a temperature change ΔT is

$$\Delta E = I \Delta R = I R_0 \alpha \Delta T \tag{3}$$

For a constant wall temperature, T_w, the local heat transfer rate at the wall from the passage of a normal shock wave over a plate is given by[40]

$$q(t) = -k_w \sqrt{u_a / 2 u_b t \nu_w}\ (T_w - T_{w,i}) S'(0) \tag{4}$$

where k_w and ν_w are the gas conductivity and kinematic viscosity at the wall temperature, $T_{w,i}$ is the insulated wall temperature, u_b and u_a are the free stream velocities before and after the normal shock, and $S'(0)$ is a coefficient tabulated in Ref. 40. By equating Eqs. (1) and (2) the value of the gage coefficient $\sqrt{(\rho C_p k)_b}/\alpha$ can be determined by

$$\frac{\alpha}{\sqrt{(\rho C_p k)_b}} = \frac{\Delta E}{I R_0 k_w (T_w - T_{w,i}) \sqrt{\pi u_a / 2 u_b \nu_w}\ S'(0)} \tag{5}$$

The heat transfer gages were calibrated over a shock Mach number range of 1.5 to 3.0, with the actual pressure rises on the surface of the plate corresponding to the pressure increases encountered in the test section flows. By this method the gage calibration contained any strain gage effects that the thin platinum film might exhibit under the pressure loading. In these calibration tests all of the electronic circuits related to each gage, including the oscilloscope used in the calibration, were also used in the actual tests in the shock tunnel.

The reduction of the temperature-time oscilloscope traces for the heat transfer gage requires the relationship between the heat transfer rate q(t) and temperature T(t), and such a relationship is given in Ref. 41 as

$$q(t) = \frac{\sqrt{\pi(\rho C_p k)_b}}{2\alpha I_0 R_0}\left[\frac{\Delta E(t)}{\sqrt{t}} + \frac{1}{\pi}\int_0^t \frac{\sqrt{\tau/t}\,\Delta E(t) - \Delta E(\tau)}{(t-\tau)^{3/2}}\,d\tau\right] \tag{6}$$

The local heat transfer rates for helium and air flows were calculated from this equation using the voltage-time traces of the heat gages and the gage coefficients determined from the calibration shock tube. A GE 605 computer was utilized to solve this equation for each heat gage trace.

3.3 Viscosity and Knudsen Number for Helium and Air

The helium viscosity relationship from Ref. 42 in terms of slugs per foot-sec. is given by

$$\mu = 7.173 \times 10^{-9}\, T^{0.647} \tag{7}$$

where T is the absolute temperature in degrees Rankine. For the pressures and temperatures encountered in the experiments the helium was treated as a perfect gas with the ratio of specific heats $\gamma = 5/3$ and the values of C_p, C_v, and R were taken as being constant.

With air as the test gas the local static temperature in the test section was approximately 30°R at a Mach number of 19. During the expansion in the nozzle the air was assumed to be in equilibrium so that the thermodynamic properties of air presented in Refs. 38 and 39 were used in the analysis. The equation for the viscosity

in slugs per foot-sec. was taken to be

$$\mu = 8.04 \times 10^{-10} \, T, \; 0 \leq T \leq 180°R \tag{8}$$

The mean free path λ, at the plate leading edge in the test section was determined for both helium and air by[43]

$$\lambda_1 = \frac{\mu_1}{0.499 \, \rho_1 \, \bar{V}_1} \tag{9}$$

where $\bar{V}_1$ is the average molecular velocity given by

$$\bar{V}_1 = \left(\frac{8RT_1}{\pi}\right)^{1/2} \tag{10}$$

For both gases the leading edge Knudsen number is defined as the ratio of the mean free path ahead of the plate to the leading edge thickness t,

$$Kn_1 = \frac{\lambda_1}{t} \tag{11}$$

It was shown in Ref. 19, for rarefied flow conditions, from the kinetic theory standpoint that the distance traveled along the plate for a time of one intermolecular collision in the free stream is given by

$$\xi_1 = M\lambda_1, \tag{12}$$

which indicates that at high flow Mach numbers the leading edge slip flow region can extend over an appreciable distance.

4.0 HEAT TRANSFER FOR A FLAT PLATE IN HYPERSONIC HELIUM FLOWS

The heat transfer rates on a flat plate were investigated initially at flow Mach numbers of 67.3 and 86.8 with helium as the test gas and the results are presented in Ref. 6 and in Fig. 2. For these tests two sets of heat gages were used to measure the local heat transfer rates in rarefied hypersonic flows. Since the densities in the test section at these very high Mach numbers were low as indicated by the mean free path length and unit Reynolds number in Table I, additional tests with helium were conducted at Mach numbers of 22.8 and 43.3 for higher density conditions in the test section to approach the continuum flow regime over the sharp flat plate as indicated in Table I by the smaller leading edge Knudsen number and higher unit Reynolds number. Another set of heat gages were used for these latest tests at lower Mach numbers. For both series of investigations to determine the local heat transfer rates, the reflected stagnation temperature was approximately 2400°R as indicated in Table I. The flow conditions tabulated in this table were based upon the free stream flows existing in the nozzle at the leading edge location of the flat plate and by the use of Eqs. (7) and (9).

Local heat transfer rates for the free stream Mach numbers of 22.8 to 86.8 were calculated by numerically integrating the voltage-time trace for each gage using Eq. (6) on the computer. These results are presented in Fig. 2 as a function of the distance from the plate leading edge for flow Mach numbers of 22.8, 43.3, 67.3, and 86.8. At the higher Mach numbers two sets of heat gages were used to measure the local heat transfer rates and the agreement between these sets of heat gages for the local heat transfer rates is very close. Since the densities in the test section at the lower Mach numbers of 22.8 and 43.3 were higher, Table I, only a single run was made at each Mach number to obtain the local heat transfer distribution over the sharp flat plate. For these tests the ratio of the wall temperature to the free stream stagnation temperature was approximately 0.22 as indicated in Table I. This low wall temperature ratio indicated highly cooled conditions for the viscous hypersonic flow over the plate.

At a Mach number of 22.8 the unit Reynolds number per inch was 66,640 and the leading edge Knudsen number was 0.555 so that the local heat transfer rate increased monotonically towards the leading edge. In the previous investigation with air at Mach numbers of 19.2 and 25.4, Ref. 5, the local heat transfer rates increased rapidly towards the leading edge for unit Reynolds number greater than 6,000 and leading edge Knudsen number less than 6 for a free stream Mach number of 25.4. Thus, with helium at this Mach

number of 22.8 the density is high enough so that the rarefied flow effects on the local heat transfer rates over the flat plate are negligible and continuum flow exists with no slip flow at the surface. At a flow Mach number of 43.3 the unit Reynolds number was 22,460 with a leading edge Knudsen number of 3.13 as presented in Table I. The local heat transfer rates for this Mach number in Fig. 2 also indicate the rapid increase in the heat transfer rates towards the leading edge which is characteristic of a continuum flow with no slip flow at the plate surface. Thus, at these lower Mach numbers the helium flow over the flat plate is in the continuum regime as indicated by the local heat transfer distributions.

For a Mach number of 67.3 the unit Reynolds number was 13,240 with leading edge Knudsen number of 8.39, Table I. The local heat transfer rate increased monotonically towards the leading edge in Fig. 2, but the rate of increase of the heat transfer rate near the leading edge is not as rapid as observed at the lower Mach numbers of 22.8 and 43.3. From the previous investigations in air at Mach numbers of 19.2 and 25.4, Ref. 5, the local heat transfer variation with distance at this flow Mach number of 67.3 would indicate that rarefied flow effects are present towards the leading edge region with consequent lower heat transfer rates than for continuum flow conditions.

For the flow Mach number of 86.8 in the test section the unit Reynolds number decreased to 8,270 and the leading edge Knudsen number increased to 17.1 as presented in Table I. At these low density conditions in the test section, the local heat transfer rates did not increase rapidly towards the leading edge in Fig. 2 compared to the lower flow Mach numbers. The decrease in the heat transfer rate with distance from the leading edge was small indicating the approach to the free molecule type of flow. In the previous investigation[5] with air at a Mach number of 25.4 the local heat transfer rate decreased slowly with the distance from the leading edge for a Knudsen number of 16.9 and unit Reynolds number of 2241, similar to that observed with helium at a Mach number of 86.8 in Fig. 2.

For these conditions in helium and air with approximately the same mean free path in the free stream or the leading edge Knudsen number of approximately 17, the variations in the local heat transfer rate with distance were similar but the unit Reynolds number for air was much less than that with helium. This difference may be possible to deduce from the consideration of the relationship between the unit Reynolds number, Mach number, and mean free path. The unit Reynolds number for both helium and air can be expressed as

$$Re/L = \frac{\rho V}{\mu} \tag{13}$$

where ρ is the density, μ is the viscosity, and V is the free stream velocity. By substituting the expression for the viscosity, Eq. (9) and using the relationship between the mean and molecular velocity and velocity of sound, Eq. (13) becomes

$$Re/L \sim \frac{M}{\lambda} \tag{14}$$

Thus, for a given mean free path the unit Reynolds number is proportional to the free stream Mach number. The ratio of the unit Reynolds number for helium at a Mach number of 86.8 and air at 25.4 for the same leading edge Knudsen number is very close to the ratio of Mach number as indicated by Eq. (14).

The local heat transfer rates were normalized with respect to the kinetic energy in the free stream at the plate leading edge and the results for the flow Mach number range of 22.8 to 86.8 are presented in Fig. 3 as a function of distance from the leading edge in terms of the free stream mean free path. For a free molecule flow with diffuse reflection at the plate surface, the local heat transfer rate would be constant along the plate as discussed in Ref. 44. And the normalized heat transfer rate for diffuse reflection is given by

$$\frac{q}{\frac{1}{2}\rho_1 u_1^3} = \frac{1}{\sqrt{2\pi\gamma}} \frac{1}{M_1} \left[1 + \frac{4}{\gamma M_1} - \frac{4R\ T_w}{u_1^2} \right] \tag{15}$$

where γ is the ratio of specific heats, 5/3, for helium. The values of this quantity for Mach numbers of 22.8 to 86.8 are presented in this figure.

At the lowest flow Mach number of 22.8 the first heat gage, x = 0.19 in., was located approximately 342 mean free paths from the plate leading edge. Because of the relatively high density conditions in the test section, as indicated in Table I, for this Mach number there are a large number of collisions between the helium atoms and the flat plate before the first heat gage location during the transit time of the flow. The distance traversed along the plate for the time of one collision in the free stream, given by Eq. (12), is 0.0126 in., which corresponds to 22.8 mean

free paths from the leading edge. For this flow condition the rarefied flow phenomena over the flat plate is restricted over the initial distance, for the time of a few collisions in the free stream, of approximately 0.025 in. Thus, the local heat transfer rates over the heat gage locations are in the continuum flow regime with no slip flow at the plate surface. And the heat transfer rate at the first heat gage location of 0.19 in., is much lower than the diffuse free molecule limit as indicated in Fig. 3. The last heat gage, $x = 12.945$ in. was located 23.5×10^4 mean free paths from the leading edge. Since the flow over the plate is in continuum flow regime for this Mach number, the normalized heat transfer rate over the plate surface did not vary appreciably.

At a flow Mach number of 43.3 the first heat gage was located at a distance of approximately 61 mean free paths from the leading edge as indicated in Fig. 3. And the distance traversed along the plate, Eq. (12), for the time of one collision in the free stream is 0.136 in. The number of collisions in the free stream for the transit time to cover the distance of 0.19 in. to the first heat gage is approximately 1.4. At this gage location the normalized heat transfer rate is much higher than the diffuse free molecule limit as indicated in this figure. The normalized heat transfer rates over the plate surface at this Mach number agree with the values observed at the lower Mach number of 22.8 for distance normalized in terms of the mean free paths. For this flow Mach number the free stream density was high enough to produce a relatively high value for the unit Reynolds number and a relatively small mean free path as is indicated in Table I. In air at a flow Mach number of 25.4 in Ref. 5 and at a Mach number of approximately 21 in Ref. 10, the normalized heat transfer rates for a sharp flat plate varied with the normalized distance at high density flow conditions similar to that observed for helium flows at Mach numbers of 22.8 and 43.3 as shown in Fig. 3.

For a flow Mach number of 67.3 the density in the test section is decreased, as presented in Table I, so that the first heat gage is located at approximately 23 mean free paths from the leading edge, and the distance traversed along the plate for the time of one collision in the stream is 0.565 in. This distance corresponds to a location between second and third heat gage on the plate. The scatter in the two sets of heat gages are small as indicated in this figure. The heat transfer rates at the plate leading edge region were much higher than the value for a free molecule flow with diffuse reflection given by Eq. (15). But for distances farther back along the plate the normalized heat transfer rates approach the levels observed at the lower Mach numbers of 22.8 and

43.3 so that enough collisions between the helium atoms and the surface have occurred to have no slip flow at the surface.

The lowest density flow conditions with the largest mean free path in the test section, Table I, existed for the highest test section Mach number of 86.8. And the normalized heat transfer rates are presented as a function of the mean free path in Fig. 3. Because of the low free stream density in the test section, there was a slightly greater scatter in the heat transfer data towards the leading edge compared to the lower Mach numbers. At this flow Mach number the first heat gage is located 11.1 mean free paths from the leading edge, and the distance traversed along the plate in the time of one collision in the free stream is approximately 1.5 in. This distance corresponds to a location slightly downstream of the sixth heat gage. The heat transfer rates over this distance are much higher than the value for the free molecule flow with diffuse reflection. Again the normalized heat transfer coefficient approached the values observed for the lower Mach numbers over the downstream portion of the plate as indicated in Fig. 3.

A number of authors have considered the hypersonic leading edge flow phenomena in the free molecule to continuum flow regime[19-28]. Most of the available theories consider the flow to be in continuum flow with slip flow at the plate surface and some of the references treat the problem from the kinetic theory concept[19-24]. The existing theories do not contain the leading edge Knudsen number explicitly in the analysis for rarefied hypersonic flow conditions. In Ref. 10 some of the existing theories have been compared with the experimental flat plate pressure and heat transfer measurements in rarefied hypersonic flow conditions.

The effects of wall temperature ratio on the surface induced pressure and local heat transfer rates on a flat plate at hypersonic Mach numbers with no slip flow were investigated by Li and Nagamatsu in Ref. 15. A similar solution concept was used by the authors to solve the noninsulated hypersonic flow over a sharp flat plate. The induced pressure near the plate leading edge was assumed to vary as $x^{-1/2}$ as originally shown in Ref. 14 and observed experimentally by a number of investigators[1,2,7-12] for hypersonic continuum flows. Besides these conditions, it was assumed that the Prandtl number of the fluid was unity and the viscosity was a linear function of the temperature. With these assumptions the hypersonic boundary layer equations were transformed into a system of ordinary differential equations. In Refs. 15 and 45 these equations were solved for the ratio of specific heats of 1.4 and 1.67 and for ratios of wall to stagnation

temperature of 0 to 2.0.

With these approximations for the similar solutions, the strong interaction between the leading edge shock wave and the viscous boundary layer on a flat plate in continuum hypersonic flow yields a theoretical heat transfer coefficient[15] given by

$$C_{h_1}\sqrt{Re_x} = D(M_1^3/\sqrt{Re_x})^{1/2} \tag{16}$$

where

$$C_h = \frac{q}{\rho u(H_5 - H_w)} \tag{17}$$

H_5 = stagnation enthalpy

H_w = wall enthalpy

$Re_x = \frac{\rho u x}{\mu}$

The Reynolds number is based upon the free stream flow condition existing at the plate leading edge location. And the expression for $D = f(\gamma, T_w/T_5)$ and its values are tabulated in Ref. 15 as a function of the ratio of the specific heats and wall temperature ratio.

Eq. (16) can also be written as

$$C_{h_1} M_1^3 = D(M_1^3/\sqrt{Re_x})^{3/2} \tag{16a}$$

and this relationship was used to correlate the experimental heat transfer data with the theoretical prediction in Fig. 4 for helium flow Mach numbers of 22.8 to 86.8. The theoretical curve in this figure was calculated for wall to stagnation temperature ratio of 0.225 over the strong interaction parameter, $\chi = M_1^3/\sqrt{Re_x}$, range of 10 to 10^4. Also, in this figure the local heat transfer coefficients for diffuse free molecule flow conditions are presented for the different free stream Mach numbers.

For the Mach 22.8 test the strong interaction parameter varied

from approximately 11 to 100 for the heat gage locations as shown in Fig. 4. And the leading edge Knudsen number was 0.555 with unit Reynolds number of 66,640, cf. Table I. For this flow condition the free stream density was high enough so that the local heat transfer coefficient varied linearly with χ with the slope close to that predicted by the Li-Nagamatsu[15] theory for the cooled wall condition and no slip flow at the surface. Even at the first heat gage location of 0.19 in. the local heat transfer coefficient was close to the theoretical slope, which indicates that the rarefied flow effects were confined very close to the leading edge region ahead of the first heat gage location. For the Mach 43.3 flow condition the strong interaction parameter χ varied from approximately 150 to 1100 over the heat gages, and the leading edge Knudsen number was 3.13 with unit Reynolds number of 22,460 as presented in Table I. Again the heat transfer coefficient varied nearly linearly with χ with the slope slightly less than that predicted by the theory as shown in Fig. 4. The heat transfer coefficient at the first heat gage location was on the linear slope. Thus, even at this Mach 43.3 flow condition the density was high enough to produce continuum flow conditions over the heat gages. Similar results were observed with air at Mach numbers of 19.2 and 25.4 in Refs. 3 - 5 where the local heat transfer coefficient agreed with the strong interaction theory of Li and Nagamatsu[15] for unit Reynolds numbers greater than approximately 15,000. In Fig. 4 the diffuse free molecule flow value is also plotted for the various test Mach numbers, and at a Mach number of 43.3 the local heat transfer rate at the first heat gage location is greater than the free molecule value.

At a test Mach number of 67.3 the leading edge Knudsen number was 8.39 with unit Reynolds number of 13,240, and over the heat gage locations the strong interaction parameter varied from approximately 740 to 6000 as indicated in Fig. 4. Over the strong interaction parameter range of 740 to approximately 2500 the local heat transfer coefficient varied nearly linearly with χ with the slope slightly less than that predicted by the Li-Nagamatsu theory[15] for the cooled wall condition. But for the strong interaction parameter range of approximately 2500 to 6000 the $M_1^3 C_h$ values depart from a straight line because of the slip flow effects as observed in Refs. 3 - 6, 10 - 12 with air at rarefied hypersonic flow Mach numbers. The departure from the linear variation is not very large in the vicinity of the leading edge, which indicates that the slip flow effects are not large at this high flow Mach number because of the reasonably high unit Reynolds number. As shown in the figure the local heat transfer rates in the vicinity of the leading edge are much greater than the diffuse free molecule value for a free stream Mach number of 67.3. Lower free stream density or lower unit Reynolds number and larger Knudsen numbers are necessary at a flow Mach number of 67.3 to achieve heat transfer rates

predicted by the diffuse free molecule flow theory.

In Fig. 4 the local heat transfer coefficients at a free stream Mach number of 86.8 are presented as a function of the strong interaction parameter χ. For this test condition the strong interaction parameter varied from approximately 2000 to 16,500 and the leading edge Knudsen number was 17.1 for a unit Reynolds number of 8,220. Over the strong interaction parameter range of 2000 to approximately 4500 the local heat transfer coefficient varied nearly linearly with χ and the slope was slightly less than that predicted by the theory[15]. Over a χ range of 4500 to 16,500 the local heat transfer coefficient departs from the linear variation, predicted theoretically for no slip flow at the surface, and towards the leading edge with high χ values the heat transfer coefficient is approaching a constant value. But the local heat transfer rates are much higher than the diffuse free molecule value for a Mach number of 86.8. The rarefied flow effects have decreased the local heat transfer rates over the forward portion of the flat plate from the theoretical prediction with no slip flow at the plate surface. For this Mach number of 86.8 much higher densities with corresponding higher unit Reynolds than 8,220 will be necessary to have continuum flow conditions over the heat gages with no slip flow at the surface. Similar results for the local heat transfer rates were observed at low density conditions with air in Refs. 3 - 6 and 10 - 12.

The normalized local heat transfer parameter $M_1^3 C_h/\chi^{3/2}$ is presented in Fig. 5 as a function of the rarefaction parameter $\bar{V}_{\infty_1} = M_1/\sqrt{Re_x}$ for the free steam Mach number range of 22.8 to 86.8. In this figure the variations of the heat transfer parameter with the rarefaction parameter are presented for the condition of diffuse free molecule flow condition over the flat plate. For the flow Mach number of 22.8 the range of the rarefaction parameter for the heat gage locations was from approximately 0.024 to 0.19, and the parameter $M_1^3 C_h/\chi^{3/2}$ does not vary much over the plate surface indicating that the slip flow effects are small. Similar results were observed in the previous figure for the variation of the heat transfer coefficient with the strong interaction parameter for this flow Mach number. The range of the rarefaction parameter for Mach number of 43.3 was from approximately 0.08 to 0.63. Again over this range of the rarefaction parameter the normalized heat transfer parameter remained nearly constant indicating very little slip flow effects over the plate surface, similar to that observed at a Mach number of 22.8. In air at a Mach number of approximately 20, the rarefaction effects became significant for the rarefaction parameter of approximately 0.3 in Refs. 5 and 10.

Over a range for the rarefaction parameter of 0.16 to 0.45 for a

free stream Mach number of 67.3, the normalized heat transfer parameter is nearly constant in Fig. 5, indicating that the slip flow effects are negligible over the aft portion of the plate. But for the range of $\bar{V}_\infty$, from 0.45 to 1.35 the local heat transfer coefficient is approaching the slope of the diffuse free molecule heat transfer rate. The magnitude of the heat transfer coefficients over this range of the rarefaction parameter is much greater than the free molecule values as shown in this figure. For this Mach number the strong interaction parameter χ varied from 740 to 6000 while the corresponding rarefaction parameter varied from 0.16 to 1.35 for the heat gage locations on the plate. The decrease in the $M_1^3 C_h/\chi^{3/2}$ with the rarefaction parameter from the constant value for the no slip condition is not large. Thus, the slip flow effects are not large over the flat plate near the leading edge, which was also indicated in Fig. 4 for the variation of the heat transfer coefficient with the strong interaction parameter. Lower density conditions are necessary at this Mach number of 67.3 to achieve greater rarefaction effects.

For a flow Mach number of 86.8 the normalized heat transfer coefficient was nearly constant for the rarefaction parameter range of 0.26 to approximately 0.58, Fig. 5. While for a Mach number of 67.3 the slip flow effects became evident for a rarefaction parameter of approximately 0.45, and for air at a Mach number of approximately 20 in Refs. 5, 6 and 10 the rarefied flow effects became noticeable for a rarefaction parameter of approximately 0.3. Hence, these experimental results for the local heat transfer rates for a sharp flat plate in air at Mach numbers of 19.2 and 25.4 and in helium at Mach numbers of 67.3 to 86.8 indicate that the value of the rarefaction parameter at which the slip flow effects begin to decrease the local heat transfer rate increases with the flow Mach number. Over a range of rarefaction parameter of 0.6 to 2.2 for the Mach number of 86.8, the normalized heat transfer parameter is approaching the slope for diffuse free molecule heat transfer values as shown in Fig. 5. But the value of the local heat transfer rate is much higher than the free molecule value.

5.0 HEAT TRANSFER IN HYPERSONIC CORNER FLOW WITH AIR AT MACH NUMBER OF 19

Two flat plates with sharp leading edges, Fig. 1, were used to investigate the local heat transfer rates in the corner region with the vertical perpendicular plate at 0, 2-1/2, and 5° angle of attack with respect to the free stream. The leading edge of both plates was in the same plane and the leading edge of the vertical plate was located 3/4 in. from the center line of the horizontal plate. Heat gages on the horizontal plate were located from 0.19 to 12.95 in. from the leading edge as shown in Fig. 1. Since the width of the sputtered platinum heat gages was approximately 0.5 in., the increase in the local heat transfer rate due to the shock wave from the vertical plate is not as large as it would be for shorter width gages. And at 5° angle of attack for the vertical plate with the leading edge fixed at 3/4 in. from the center line the gages located towards the end of the horizontal plate are covered by the vertical plate as shown in Fig. 1.

The complete model was mounted on a sting in the shock tunnel with the leading edge of the plate located slightly downstream of the 24 in. diameter conical nozzle[35,36]. For these tests the combustion driver technique was used to produce the heated and compressed air at the end of the 103 foot long driven tube. To minimize the real gas effects the air was heated to a reflected stagnation temperature of approximately 2300°R at the entrance to the conical nozzle. The hypersonic corner flow phenomenon was investigated for rarefied to continuum flow conditions, which were determined in Ref. 5 for air at Mach numbers of 19.2 and 25.4. The reflected stagnation pressures of approximately 80, 296, and 1320 psia with corresponding unit Reynolds number of approximately 1,000, 3,900, and 17,000 respectively were selected as presented in Table II. The heat gages were calibrated in the 8 in. shock tube before and after the tests in the shock tunnel. An impact pressure probe, located in the plane of the flat plate leading edge, Fig. 1a, was used to determine the flow Mach number for equilibrium expansion in the nozzle[36]. For these tests the ratio of the model wall to reflected stagnation temperature was approximately 0.23 as presented in Table II.

The local heat transfer rates are presented in Figs. 6a, 7a, and 8a as a function of the distance from the leading edge for the vertical plate at angles of attack of 0, 2-1/2, and 5° at reservoir pressures of approximately 80, 296, and 1320 psia. In Fig. 6a the surface heating rates are presented for reflected stagnation pressure of approximately 80 psia, stagnation temperature of approximately 2385°R, and flow Mach number of 19. For these test conditions

the unit Reynolds number was approximately 1,000 with a leading edge Knudsen number of approximately 27 as presented in Table II. Previous investigations[5] with air at Mach numbers of 19.2 and 25.4 indicated that the rarefied flow effects on the surface heat transfer were large at these low unit Reynolds numbers. With only the horizontal plate the local heat transfer rate did not increase rapidly towards the leading edge because of the rarefied flow effects, and the heat transfer rates are tending to approach a plateau, which is the case for free molecule flow conditions.

By placing the vertical plate at 0° angle of attack and 3/4 in. from the center line of the horizontal plate, the local heat transfer rates over the initial distance of approximately 1 in. from the leading edge were close to the values for the horizontal plate alone as shown in Fig. 6a. But for the heat gages located farther downstream, the local heat transfer rates were greater than the values for the horizontal plate alone with the greatest increase occurring at approximately 2.1 in. from the leading edge. Similar results were observed in Ref. 6 with the vertical plate located 0.5 in. from the center line. The increase in the local heat transfer rate at this location was approximately 30 percent higher than that for the plate alone. This increase in the local heat transfer rate is due to the interaction of the shock wave from the vertical plate with the boundary layer on the horizontal plate. Similar increases in the local heat transfer rates in the corner region were observed by other authors[30-32,46,47] in hypersonic flows with air and helium. By increasing the angle of attack of the vertical plate to 2-1/2 and 5°, which increases the strength of the shock wave, the local heat transfer rates over most of the horizontal plate were increased as indicated in Fig. 6a. The increase started closer to the leading edge because of the stronger shock wave from the vertical plate interacting with the horizontal plate boundary layer. For both 2-1/2 and 5° the greatest increase over the value for the heat transfer rate on the horizontal plate alone occurred at approximately 1.8 in. from the leading edge. The increase in the heating rates were approximately 65 and 71 percent at angle of attack of 2-1/2 and 5° compared to the horizontal plate alone. For an angle of attack of 2-1/2° the local heat transfer rates were higher than the values for the 0° angle of attack over the initial 5 in. of the plate. But with the vertical plate at an angle of attack of 5° the local heat transfer rates were higher than values for the 0° angle of attack case over the initial 3.2 in., and for larger distances from the leading edge the local heat transfer rates became less than the horizontal plate by itself. This variation of the local heat transfer rate is due to the complicated corner flow phenomena[29,47] and the fact that the vertical plate is over the

last two heat gages as shown in Fig. 1b.

The heat transfer rates with vertical plates at angles of attack of 0, 2-1/2, and 5° are presented in Figs. 7a and 8a for reflected stagnation pressures of approximately 296 and 1320 psia with leading edge Knudsen numbers of approximately 7.15 and 1.65 respectively as presented in Table II. For a reservoir pressure of 296 and unit Reynolds number of approximately 3,900 and a Mach number of 19, it was observed in Ref. 5 that the rarefied flow effects existed. The local heat transfer rates increased towards the leading edge with only the horizontal plate as in Fig. 7a. With the vertical plate at zero degree angle of attack and 3/4 in. from the center line of the horizontal plate, the local heat transfer rate did not increase over the initial 1.2 in. of the plate compared to the case without the vertical plate. Also, because of the higher free stream density and thinner boundary layer on the plate the increase in the local heat transfer rate in the corner region was not as large as observed at the lower density conditions, Fig. 6a. Similar results for the heat transfer rate were obtained in the corner region at the higher pressure of 1300 psia and unit Reynolds number of approximately 17,000 and vertical plate at 0° angle of attack as indicated in Fig. 8a. Because of the high Reynolds number the flow over the flat plate was in the continuum regime as observed in Ref. 5 with the local heat transfer rate increasing rapidly towards the leading edge. The increase in the local heat transfer rate from that of the horizontal plate alone was small. And the local heat transfer rate over the initial 1.1 in. was close to that of the horizontal plate by itself. This small increase in the heating rate with the vertical plate at zero degree angle of attack is due to the thinner boundary layer existing on both horizontal and vertical plates in the corner region.

For the vertical plate at an angle of attack of 2-1/2° the local heat transfer rates over the horizontal plate increased over that of the values existing for the vertical plate at zero degree angle of attack for both reflected stagnation pressures of 296 and 1300 psia as indicated in Figs. 7a and 8a. But the increase in the heating rate at 296 psia was greater than that observed at the higher pressure of 1300 psia for continuum flow conditions. But with the vertical plate at an angle of attack of 5° the local heat transfer rate increased appreciably over that of the horizontal plate alone for both reflected reservoir pressures of 296 and 1300 psia. Evidently the strong shock wave from the vertical plate was effective in producing an appreciable change in the boundary layer on the horizontal plate with a corresponding increase in the heating rate in the corner region as observed in Refs. 30, 31, and 47.

In Figs. 6b, 7b, and 8b the normalized heat transfer rates in the corner region are presented as a function of the distance in terms of the mean free path in the test section for reflected stagnation pressures of approximately 80, 296, and 1300 psia. At a pressure of 80 psia with unit Reynolds number of approximately 1,000 and leading edge Knudsen number of approximately 27, the normalized heat transfer rate for the horizontal plate by itself is tending to approach a limiting value towards the leading edge. The first heat gage was located approximately 7 mean free paths and the last gage was approximately 500 mean free paths. Because of the low density flow conditions the slip flow effects are appreciable over most of the plate surface as observed previously in Ref. 5. With the addition of the vertical plate 3/4 in. from the center line at zero degree angle of attack, the shock wave from the vertical plate began to increase the local heating at approximately 40 mean free paths from the leading edge as indicated in Fig. 6b, and the greatest increase over that of the horizontal plate alone occurred at a distance of approximately 70 mean free paths. At angles of attack of 2-1/2 and 5° for the vertical plate, the horizontal heat transfer rate was increased from approximately 15 mean free paths from the leading edge with the largest increase occurring at approximately 60 mean free paths for both angles. At approximately 150 mean free paths from the leading edge the normalized heat transfer rates were about the same for the three angle of attacks for the vertical plate.

For the reflected stagnation pressure of approximately 296 psi with unit Reynolds number of 3900, the normalized heat transfer rates for the horizontal plate alone decreased continuously with the distance from the leading edge as indicated in Fig. 7b and observed in Ref. 5. The heat gages on the horizontal plate were located over 26 to 1800 mean free paths from the leading edge. With the vertical plate at zero degree angle of attack the local heat transfer rates were very close to that of the horizontal plate alone over the initial distance of 200 mean free paths, and downstream of this location the heat transfer rates were higher than with only the horizontal plate. For angles of attack of 2-1/2 and 5° for the vertical plate the heat transfer rates were increased over the gages located approximately 150 mean free paths from the leading edge. And the normalized heat transfer rates were about the same at a location 600 mean free paths from the leading edge.

The normalized heat transfer rates were obtained over the horizontal plate for a distance of 115 to 8000 mean free paths from the leading edge for a reflected stagnation pressure of approximately 1300 psia in Fig. 8b. For the horizontal plate alone the normalized heat transfer rates decreased monotonically with the distance and

similar results were obtained in Ref. 5 for high density conditions of continuum flow. With the vertical plate at 0, 2-1/2, and 5° angles of attack, the normalized heat transfer rates were very close to that observed for the horizontal plate alone over the initial distance of approximately 700 mean free paths from the leading edge. And the increase in the heat transfer rates for the angles of attack of 0 and 2-1/2 were approximately the same at this high density flow conditions. But the 5° angle of attack increased the local heat transfer rates the greatest amount and the normalized heat transfer rates were approximately the same for the three angles of attack at a distance of 4500 mean free paths from the leading edge.

In Figs. 6c, 7c, and 8c the local heat transfer coefficient is plotted as a function of the strong interaction parameter with the vertical plate at angles of attack of 0, 2-1/2, and 5° for reflected reservoir pressures of 80, 296, and 1320 psia with flow Mach number of 19. At the lowest reservoir pressure of 80 psia the strong interaction parameter varied from 58 to 500 over the heat gages on the horizontal plate, and the heat transfer coefficients in the corner flow region are presented in Fig. 6c. With the horizontal plate alone the heat transfer rates over the forward portion of the flat plate were much lower than the strong interaction theory of Li and Nagamatsu[14,15] for no slip flow at the plate surface. Only towards the aft portion of the flat plate are the local heat transfer rates approaching the theoretical values. Similar large decreases in the local heat transfer rates in rarefied hypersonic flows at Mach numbers of 19.2 and 25.4 were observed in Ref. 5. By placing the vertical plate at zero degree angle of attack and 3/4 in. from the center line, the local heat transfer coefficient approached the theoretical values for the range of interaction parameter of 60 to 150, and for higher values of χ the local heat transfer rates were much less than the theoretical predictions due to slip flow effects. With the vertical plate at angles of attack of 2-1/2 and 5°, the local heat transfer coefficients were higher than for the horizontal plate alone. At these higher angles of attack the influence of the shock wave from the vertical plate was felt even towards the leading edge region as indicated in Fig. 6c.

For a reflected stagnation pressure of approximately 296 psia, the strong interaction parameter varied from 31 to 250 over the heat gage locations as indicated in Fig. 7c. The local heat transfer coefficient for the horizontal plate alone approached the strong interaction predictions for the range of χ of 31 to approximately 70, and for larger values of χ the local heat transfer coefficients became less than the theoretical values due to the

rarefied flow effects as observed in Refs. 5 and 6. Over the forward portion of the flat plate, χ range of 250 to 105, the local heat transfer coefficients with the vertical plate at angles of attack of 0, 2-1/2, and 5° were close to the values observed for the horizontal plate alone. But for positions farther back on the horizontal plate the local heat transfer rates with angle of attack for the vertical plate were higher than the horizontal plate alone and the greatest increase occurred for the 5° angle of attack.

At the highest pressure of 1320 psia used in the present investigation the strong interaction parameter over the heat gages varied from approximately 14 to 120 for a Mach number of 19.1 in Fig. 8c. The unit Reynolds number for this test condition was approximately 17,200 with leading edge Knudsen number of approximately 1.65 as presented in Table II. It was observed in previous investigations Refs. 5 and 6 with air at Mach numbers of 19.2 and 25.4 that the rarefied flow effects on the local heat transfer rates were negligible for unit Reynolds numbers greater than approximately 15,000. The local heat transfer rates for the horizontal plate alone were very close to the values predicted by the strong interaction theory of Li and Nagamatsu[14,15] for the cooled wall condition. Because of the high density in the free stream with continuum flow conditions, the local heat transfer rates with the vertical plate at angles of attack of 0, 2-1/2 and 5° were very close to the values observed with the horizontal plate alone over the χ range of 60 to 120. This phenomenon was due to the thin boundary layers on the horizontal and vertical plates at high density conditions. Downstream of this location on the plate for χ values less than 60 the local heat transfer coefficients were increased with the greatest increase occurring for the 5° angle of attack.

The dependence of the heat transfer coefficient on Mach number and Reynolds number can be removed in the strong interaction regime by dividing M^3C_h by $\chi^{3/2}$ as seen from Eq. (16a). Any departure from a constant value of $M^3C_h/\chi^{3/2}$, which depends upon the ratio of specific heats for the gas, the ratio of the wall to stagnation temperatures, and the strong interaction flow with no slip flow at the surface would indicate the beginning of the rarefied flow effects. In Figs. 6d, 7d, and 8d the local heat transfer parameter $M^3C_h/\chi^{3/2}$ is presented as a function of the rarefaction parameter $\bar{V}_\infty = M_1/\sqrt{Re_x}$ for reservoir pressures of 80, 296, and 1320 psia respectively with and without the vertical plate. The normalized heat transfer coefficients are presented in Fig. 6d for the reservoir pressure of 80 psia. Over the heat gage locations on the horizontal plate the rarefaction parameter varied from 0.16 to 1.4. Without the vertical plate the normalized heat transfer

coefficients were nearly constant over the rarefaction parameter range of 0.16 to approximately 0.3 before decreasing with higher values of $\bar{V}_\infty$. This decrease is caused by the slip flow effects in rarefied hypersonic flow as observed in Refs. 3 - 6, 10, 11. The normalized heat transfer coefficients increased with the vertical plate at angles of attack of 0, 2-1/2, and 5° as shown in Fig. 6d. And the effects of the shock wave and boundary layer on the vertical plate increased the heat transfer rates close to the leading edge of the horizontal plate. The effects of the vertical plate at angles of attack of 2-1/2 and 5° on the local heat transfer rates were approximately the same over the plate surface.

For a reservoir pressure of 296 psia the rarefaction parameter over the heat gages varied from 0.084 to 0.7 as shown in Fig. 7d. Because of the higher reservoir pressure the rarefied flow effects have been decreased for the horizontal plate alone as compared with the lower reservoir pressure, Fig. 6d. In Refs. 5 and 6 the local heat transfer coefficients varied with the rarefaction parameter at Mach numbers of 19.2 and 25.4 similar to that observed in the present investigation. The addition of the vertical plate at angles of attack did not appreciably effect the heat transfer rates over the forward portion of the horizontal plate, but further back in the corner region the local heat transfer rates were increased. The maximum increase in the local heat transfer rate due to the vertical plate was approximately the same for angles of attack of 0, 2-1/2, and 5° as shown in this figure.

For a reservoir pressure of 1320 psia the rarefaction parameter varied from 0.04 to 0.33 over the heat gage locations as shown in Fig. 8d. At this reservoir pressure the unit Reynolds number was approximately 17,200 as presented in Table II, and in Refs. 5 and 6 it was observed that the rarefied flow effects were negligible for unit Reynolds numbers greater than 15,000 for flow Mach numbers of 19.2 and 25.4. Thus, the normalized heat transfer coefficient did not vary appreciably over the horizontal flat plate by itself, indicating that the flow was in the strong interaction regime with no slip flow at the surface. Over most of the forward portion of the horizontal flat plate the local heat transfer rates for the vertical plate at angle of attacks of 0, 2-1/2, and 5° were close to that observed with only the horizontal plate. Farther downstream from the plate leading edge the increase in the normalized heat transfer coefficient was a function of the angle of attack of the vertical plate, Fig. 8d. Similar increase in the local heat transfer rate in the corner flow region with angle of attack of the vertical plate was observed in Refs. 6, 30 - 32, 46, 47. Further investigations must be conducted to determine the complicated flow phenomenon present in the corner region in hypersonic flows.

6.0 CONCLUSIONS

Surface heat transfer rates were measured on a sharp flat plate at zero angle of attack with helium over a Mach number range of 22.8 to 86.8 in a hypersonic shock tunnel. For these Mach numbers the strong interaction parameter, $\chi = M_1^3/\sqrt{Re_x}$, varied from 11 to 16,000. The leading edge Knudsen number varied from 0.56 to 17.1 and the unit Reynolds number varied from 66,600 to 8,270 for the flow Mach number range.

The local heat transfer rates increased towards the leading edge for the lower Mach numbers with continuum flow over the flat plate. But at the higher Mach numbers the local heat transfer rates did not increase appreciably towards the leading edge because of the large rarefied flow effects with slip flow on the plate surface. It required a distance along the plate of approximately 70 mean free paths to obtain no slip flow at the plate surface.

For flow Mach numbers of 22.8 and 43.3 the local heat transfer coefficient increased with the strong interaction parameter at a rate very close to that predicted by the strong interaction theory of Li and Nagamatsu with no slip flow at the plate surface. The unit Reynolds number for these Mach numbers were 66,600 and 22,460 respectively. At Mach numbers of 67.3 and 86.8 with lower density conditions, the local heat transfer coefficient increased with the strong interaction parameter downstream of the leading edge region as predicted by the strong interaction theory. And at a Mach number of 86.8 with unit Reynolds number of 8,270 the local heat transfer rates were much less than the theoretical values because of the slip flow at the surface.

The experimental heat transfer data when plotted as a function of the rarefaction parameter, $\bar{V}_{\infty_1} = M_1/\sqrt{Re_x}$, indicated that slip flow effects were negligible for flow Mach numbers of 22.8 and 43.3. But for Mach numbers of 67.3 and 86.8 the rarefied flow phenomena began to be noticeable for the values of the rarefaction parameter of approximately 0.4 and 0.6 respectively. These values are much higher than those observed with air at Mach numbers of 19.2 and 25.4 for the beginning of the rarefied flow phenomena.

The local heat transfer rates in the corner flow region produced by the intersection of two perpendicular plates with sharp leading edges were determined with air at a Mach number of 19 for various flow density in the test section. The strength of the shock wave from the vertical plate was varied by adjusting the angle of attack from 0 to 5°. For these test conditions the unit Reynolds numbers were approximately 1,000 to 17,200 in the free stream, and the leading edge Knudsen numbers were approximately 1.6 to 27. The

strong interaction parameter varied from 14 to 500.

At the low density flow conditions, the local heat transfer rates were increased approximately 70 percent in the corner region for an angle of attack of 5° for the vertical plate located 0.75 in. from the center line of the horizontal plate. At higher density conditions in the test section the local heat transfer rates in the corner flow region were increased but not as much as for the lower densities with rarefied flow.

The upstream influence on the local heat transfer rate on the horizontal plate due to the shock wave and boundary layer on the vertical plate at different angle of attack was decreased with increasing density in the test section. For the range of unit Reynolds number investigated the local heat transfer rate on the horizontal plate increased with the angle of attack of the vertical plate.

At the highest unit Reynolds number of 17,200 and a Mach number of 19.1, the local heat transfer rates for the horizontal plate alone agreed very closely with the strong interaction theory of Li and Nagamatsu for the cooled wall condition. With the addition of the vertical plate at different angles of attack, the local heat transfer rates in the corner region downstream of the leading edge were greater than the theoretical values.

For the lowest unit Reynolds number of approximately 1000 the local heat transfer rates on the horizontal plate alone were an order of magnitude less than that predicted by the strong interaction theory. The addition of the vertical plate at various angles of attack increased the local heat transfer rates, which approached the theoretical values over the downstream portion of the flat plate.

The rarefied hypersonic flow effects on the local heat transfer rates in the corner region were largest for low density flow conditions. And the angle of attack of the vertical plate increased the local heat transfer rates in the corner region downstream of the leading edge. Further analytical and experimental investigations must be conducted to increase the knowledge regarding the hypersonic corner flow phenomena.

REFERENCES

1. Nagamatsu, H.T. and Sheer, R.E., Jr., "Hypersonic Shock Wave Boundary Layer Interaction and Leading Edge Slip," ARS Jour., Vol. 30, No. 5, p. 454 (1960).

2. Nagamatsu, H.T., Sheer, R.E., Jr., and Schmidt, J.R., "High Temperature Rarefied Hypersonic Flow Over a Flat Plate," ARS Jour., Vol. 31, No. 7, p. 902 (1961).

3. Nagamatsu, H.T., Weil, J.A., and Sheer, R.E., Jr., "Heat Transfer to a Flat Plate in High Temperature Rarefied Ultra-high Mach Number Flow," ARS Jour., Vol. 32, p. 533 (1962).

4. Nagamatsu, H.T., Wisler, D.C., and Sheer, R.E., Jr., "Continuum to Free Molecule Flow in Vicinity of Leading Edge of a Flat Plate at Mach Numbers of 19.4 and 24.1," Sixth International Symposium on Rarefied Gas Dynamics, Vol. 1, p. 209, Mass. Inst. of Tech., July 1968.

5. Nagamatsu, H.T., Pettit, W.T., and Sheer, R.E., Jr., "Heat Transfer on a Flat Plate in Continuum to Rarefied Hypersonic Flow at Mach Numbers of 19.2 and 25.4," NASA Contractor Rept. NASA CR-1692 (1970).

6. Nagamatsu, H.T., Sheer, R.E., Jr., and Pettit, W.T., "Heat Transfer on a Flat Plate in Helium at Mach Numbers 67.3 and 86.8 and in Hypersonic Corner Flow with Air at Mach Number of 19," General Electric Res. and Dev. Ctr. Rept. No. 70-C-392 (1970) and also NASA Contractor Report (In Process).

7. Laurman, J.A., "The Effects of Slip Flow on Induced Pressures," J. Aero. Space Sci., Vol. 26, No. 1, p. 53 (1959).

8. McCroskey, W.J., Bogdonoff, S.M., and McDougall, J.G., "An Experimental Model for the Sharp Flat Plate in Rarefied Hypersonic Flow," AIAA J., Vol. 4, No. 9, p. 1580 (1966).

9. Becker, M. and Boylan, D.E., "Experimental Flow Field Investigations Near the Sharp Leading Edge of a Cooled Flat Plate in a Hypersonic Low Density Flow," Rarefied Gas Dynamics, C.L. Brudin, Ed. Academic Press Inc., New York, (1967) pp. 993-1014.

10. Vidal, R.J. and Bartz, J.A., "Surface Measurements on Sharp Flat Plates and Wedges in Low Density Hypersonic Flow," Cornell Aero. Lab. Rept. No. AF-2041-A-2 (1968).

11. Metcalf, S.C., Lillicrap, D.C., and Berry, C.J., "A Study of the Effect of Surface Condition on the Shock Layer Development Over Sharp Edged Shapes in Low Reynolds Number High Speed Flow," Rarefied Gas Dynamics, Academic Press Inc., New York (1969), pp. 619-634.

12. Vidal, R.J., Bartz, J.A., and Merritt, G.E., "Flowfield Surveys in the Hypersonic Viscous Shock Layer on a Sharp Flat Plate," Cornell Aero. Lab., Rept. No. AF-2919-A-1 (1970).

13. Shen, S.F., "An Estimate of Viscous Effect on the Hypersonic Flow Over an Insulated Wedge," J. Math. Phys., Vol. 31, p. 192 (1952).

14. Li, T.Y. and Nagamatsu, H.T., "Shock-Wave Effects on the Laminar Skin Friction of an Insulated Flat Plate at Hypersonic Speeds," J. Aero. Sci., Vol. 20, No. 5, p. 345 (1953).

15. Li, T.Y. and Nagamatsu, H.T., "Hypersonic Viscous Flow on Noninsulated Flat Plate," Proc. Fourth Midwestern Conf. on Fluid Mechanics, Purdue Eng. Res. Series No. 128, p. 273 (1955).

16. Lees, L., "On the Boundary Layer Equations in Hypersonic Viscous Flow and Their Approximate Solutions," J. Aero. Sci., Vol. 20, No. 2, p. 143 (1953).

17. Cheng, H.K., Hall, J.G., Golian, T.C., Hertzberg, A., "Boundary Layer Displacement and Leading Edge Bluntness Effects in High Temperature Flow," J. Aero. Sci., Vol. 28, p. 353 (1961).

18. Stewartson, K., "On the Motion of a Flat Plate at High Speeds in a Viscous Compressible Fluid II. Steady Motion," J. Aero. Sci., Vol. 22, No. 5, p. 305 (1955).

19. Nagamatsu, H.T. and Li, T.Y., "Hypersonic Flow Near the Leading Edge of a Flat Plate," Phys. Fluid, Vol. 3, p. 140 (1960).

20. Charwat, A.F., "Molecular Flow Study of Hypersonic Sharp Leading Edge Interaction," Rarefied Gas Dynamics, Academic Press Inc., New York (1961).

21. Bird, G.A., "The Structure of Rarefied Gas Flows Past Simple Aerodynamic Shapes," J. Fluid Mech., Vol. 36, Part 3, p. 571 (1969).

22. Vogenitz, F.W., Broadwell, J.E., and Bird, G.A., "Leading Edge Flow by the Monte Carlo Direct Simulation Technique," AIAA Paper No. 69-141 (1969).

23. Vogenitz, F.W. and Takata, G.Y., "Rarefied Hypersonic Flow About Cones and Flat Plates by Monte Carlo Simulation," AIAA Jour., Vol. 9, No. 1, p. 94 (1971).

24. Huang, A.B. and Hwang, P.F., "The Supersonic Leading Edge Problem According to the Ellipsoidal Model," AIAA Paper No. 69-652 (1969).

25. Chow, W.L., "Hypersonic Rarefied Flow Past the Sharp Leading Edge of a Flat Plate," AIAA Jour., Vol. 5, No. 9, p. 1549 (1967).

26. Shorestein, M.L. and Probstein, R.F., "The Hypersonic Leading Edge Problem," AIAA Jour., Vol. 6, No. 10, p. 1898 (1968).

27. Rudman, S. and Rubin, S.G., "Hypersonic Viscous Flow Over Slender Bodies with Sharp Leading Edges," AIAA Jour., Vol. 6, No. 10, p. 1883 (1968).

28. Eilers, R.E., "Hypersonic Rarefied Gas Flow Past Two-Dimensional Slender Bodies," Ph.D. Thesis, Univ. of Ill. (1969).

29. Charwat, A.F. and Redekeopp, L.G., "Supersonic Interference Flow Along the Corner Intersecting Wedges," AIAA Jour., Vol. 5, No. 3, p. 480 (1967).

30. Stainback, P.C., "Heat Transfer Measurements at a Mach Number of 8 in the Vicinity of a 90° Interior Corner Aligned with the Free Stream Velocity," NASA TN D-2417 (1964).

31. Stainback, P.C. and Weinstein, L.M., "Aerodynamic Heating in the Vicinity of Corners at Hypersonic Speeds," NASA TN D-4130 (1967).

32. Nardo, C.T. and Cresci, R.J., "Experimental Measurements of Hypersonic Corner Flow," Polytechnic Inst. of Brooklyn, Rept. No. 69-1 (1969).

33. Pal, A. and Rubin, S.G., "Viscous Flow Along a Corner Part I. Asymptotic Features of the Corner Layer Equations," Polytechnic Inst. of Brooklyn, Rept. No. 69-18 (1969).

34. Korkegi, R.H., "Viscous Interactions and Flight at High Mach Numbers," AIAA Paper No. 70-781 (1970).

35. Nagamatsu, H.T., Geiger, R.E., and Sheer, R.E., Jr., "Hypersonic Shock Tunnel," ARS Jour., Vol. 29, No. 5, p. 332 (1959).

36. Nagamatsu, H.T., Workman, J.B., and Sheer, R.E., Jr., "Hypersonic Nozzle Expansion with Air Atom Recombination Present," J. Aero. Sci., Vol. 28, p. 833 (1961).

37. Nagamatsu, H.T., Sheer, R.E., Jr., and Weil, J.A., "Improvements in Hypersonic Technique and Instrumentation," General Electric Res. Lab. Rept. 62-RL-3107C (1962).

38. Gilmore, F.R., "Equilibrium Composition and Thermodynamic Properties of Air to 24,000°K," Rand Corp. Rept. RM-1543 (1953).

39. Hilsenrath, J. and Beckett, C.W., "Tables of Thermodynamic Properties of Argon-Free Air to 15,000°K," Arnold Eng. Dev. Ctr., TN56-12 (1956).

40. Mirels, H., "Laminar Boundary Layer Behind Shock Advancing Into Stationary Fluids," NACA TN 3401 (1955).

41. Carslow, H.S. and Jaeger, J.C., Conduction of Heat in Solids, Univ. Press, Oxford (1950).

42. Mueller, J.N., "Equations, Tables, and Figures for Use in the Analysis of Helium at Supersonic and Hypersonic Speeds," NACA TN 4063 (1957).

43. Kennard, E.H., Kinetic Theory of Gases, McGraw-Hill Book Co., Inc., New York (1938).

44. Patterson, G.N., Molecular Flow of Gases, John Wiley & Sons, Inc., New York (1956).

45. Li, T.Y. and Nagamatsu, H.T., "Similar Solutions of the Compressible Boundary Layer Equations," J. Aero. Sci., Vol. 22, No. 9, p. 607 (1955).

46. Bertram, M.H. and Henderson, A., Jr., "Some Recent Research with Viscous Interacting Flow in Hypersonic Streams," Viscous Interaction Phenomena in Supersonic and Hypersonic Flow, Univ. of Dayton Press (1970).

47. Watson, R.D. and Weinstein, L.M., "A Study of Hypersonic Corner Flow Interactions," Presented at AIAA Aerospace Sciences Meeting, Jan. 1970.

TABLE I

CONDITIONS FOR HELIUM TESTS

Run	P_5 Psia	T_5 °R	T_w/T_5	M_1	Re/in.	λ_1 In. × 10^3	Kn_1
2401	1256	2450	0.216	22.8	66,640	0.555	0.555
2400	1256	2450	0.216	43.3	22,460	3.128	3.13
2372 2387	1336	2280	0.237	67.3	13,240	8.39	8.39
2371 2386	1346	2280	0.237	86.8	8,270	17.1	17.1

TABLE II

CONDITIONS FOR CORNER AIR FLOW TESTS

Run	P_5 Psia	T_5 °R	T_w/T_5	Angle Attack	M_1	Re/in.	λ_1 In. × 10^3	Kn_1
2405	84.8	2412	.220	--	19	1,082	26.1	26.1
2408	78.5	2385	.222	0°	19	1,019	27.7	27.7
2409	76.5	2385	.222	2.5°	19	993	28.4	28.4
2412	81.0	2385	.222	5°	19	1,051	26.9	26.9
2406	289	2295	.231	--	19.1	3,913	7.25	7.25
2407	294	2295	.231	0°	19.1	3,980	7.13	7.13
2410	309	2385	.222	2.5°	19.1	3,949	7.19	7.19
2411	292	2295	.231	5°	19.1	3,953	7.18	7.18
2416	1346	2340	.226	--	19.1	17,700	1.60	1.60
2415	1311	2340	.226	0°	19.1	17,240	1.65	1.65
2414	1246	2295	.231	2.5°	19.1	16,870	1.68	1.68
2413	1371	2385	.222	5°	19.1	17,520	1.62	1.62

FIG. 1a PHOTOGRAPH OF FLAT PLATE HEAT TRANSFER MODEL WITH ADJUSTABLE ANGLE OF ATTACK VERTICAL PLATE.

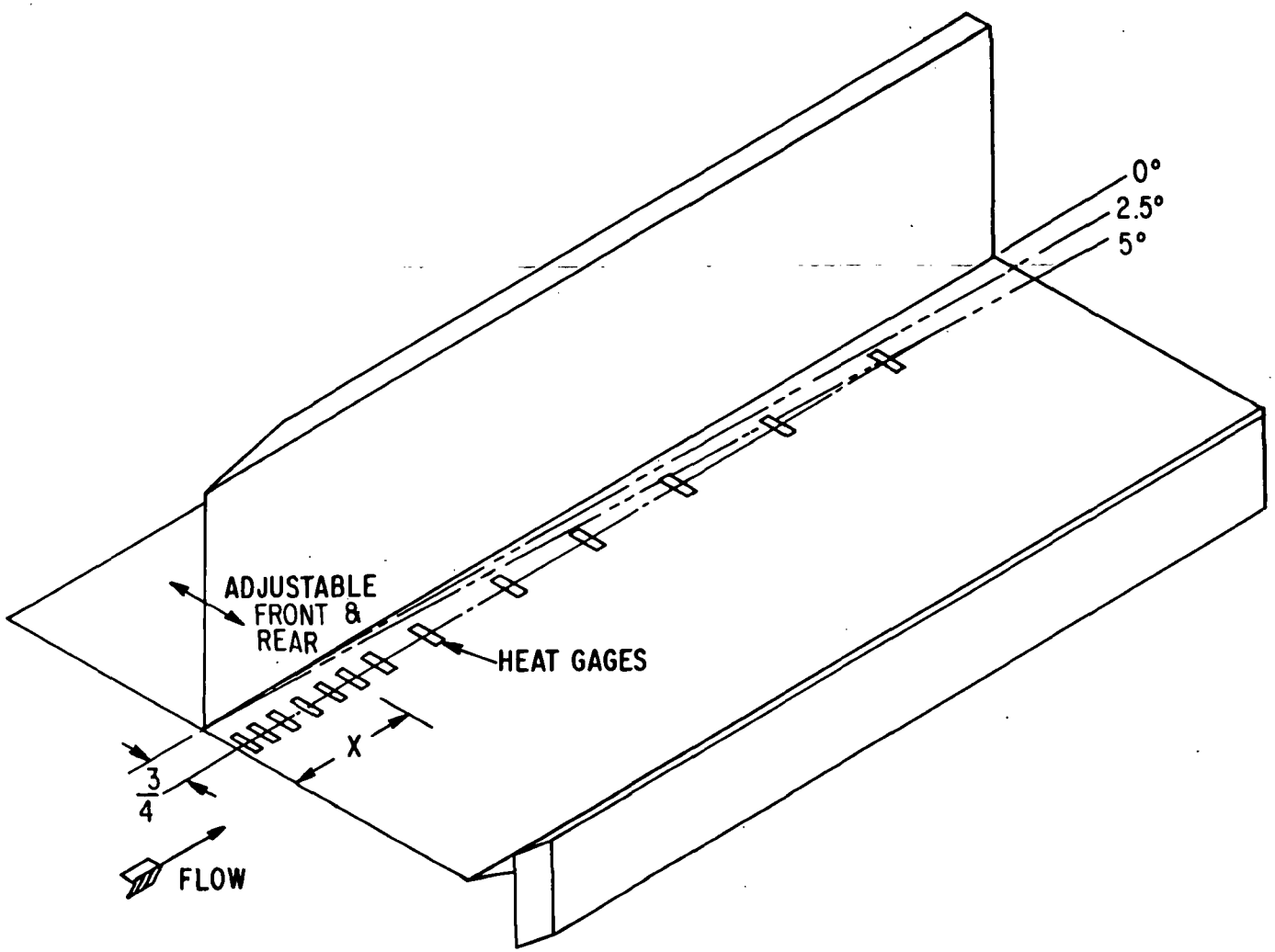

FIG. 1b SCHEMATIC OF FLAT PLATE HEAT TRANSFER MODEL FOR CORNER FLOW ARRANGEMENT

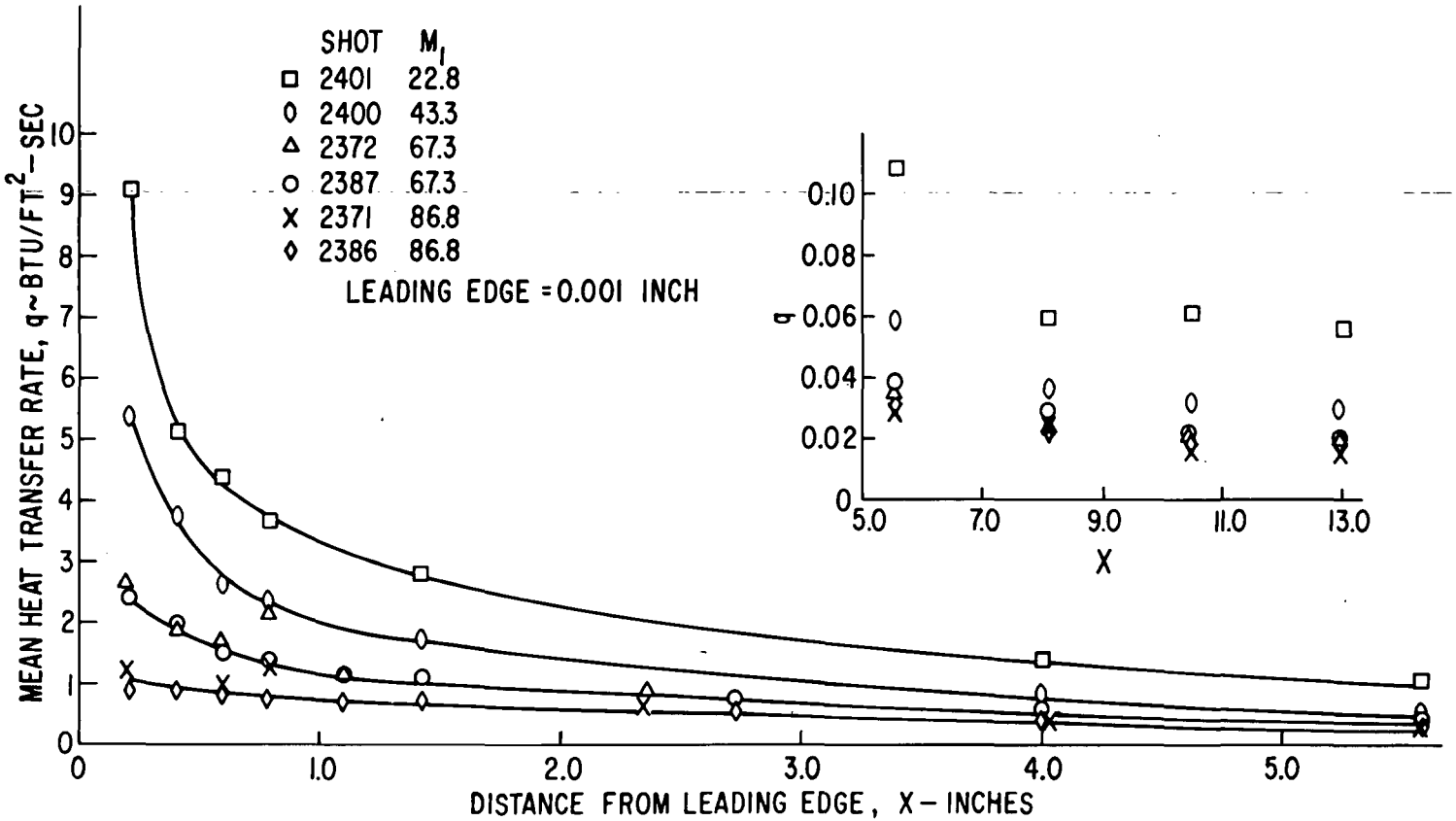

FIG. 2 HEAT TRANSFER RATE DISTRIBUTION ALONG THE PLATE WITH HELIUM, M_1 = 22.8 TO 86.8

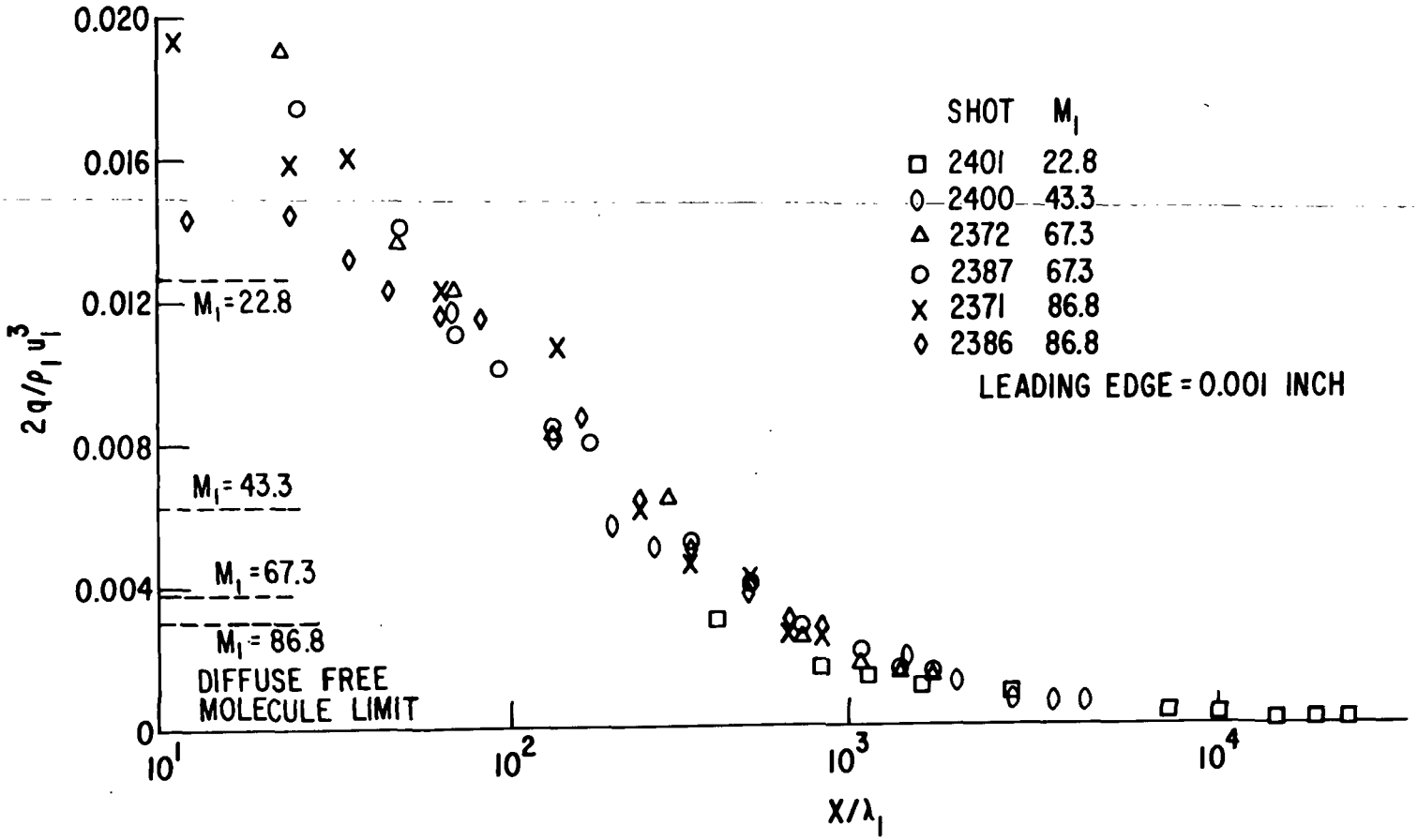

FIG.3 NORMALIZED HEAT TRANSFER RATE vs DISTANCE ALONG PLATE IN MEAN FREE PATHS WITH HELIUM, M_1 =22.8 TO 86.8

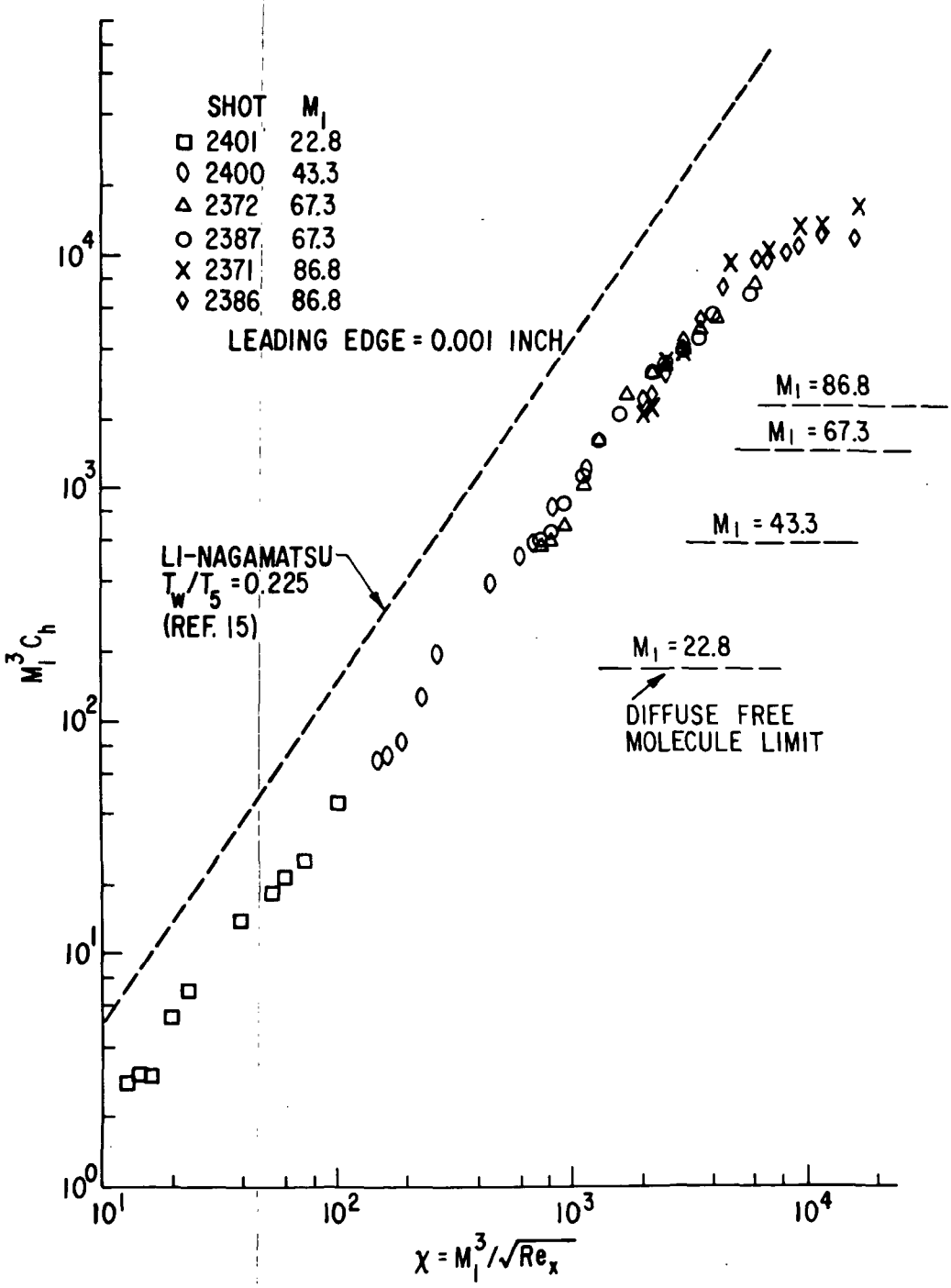

FIG.4 HEAT TRANSFER COEFFICIENT AS FUNCTION OF STRONG INTERACTION PARAMETER WITH HELIUM, M_1 =22.8 TO 86.8

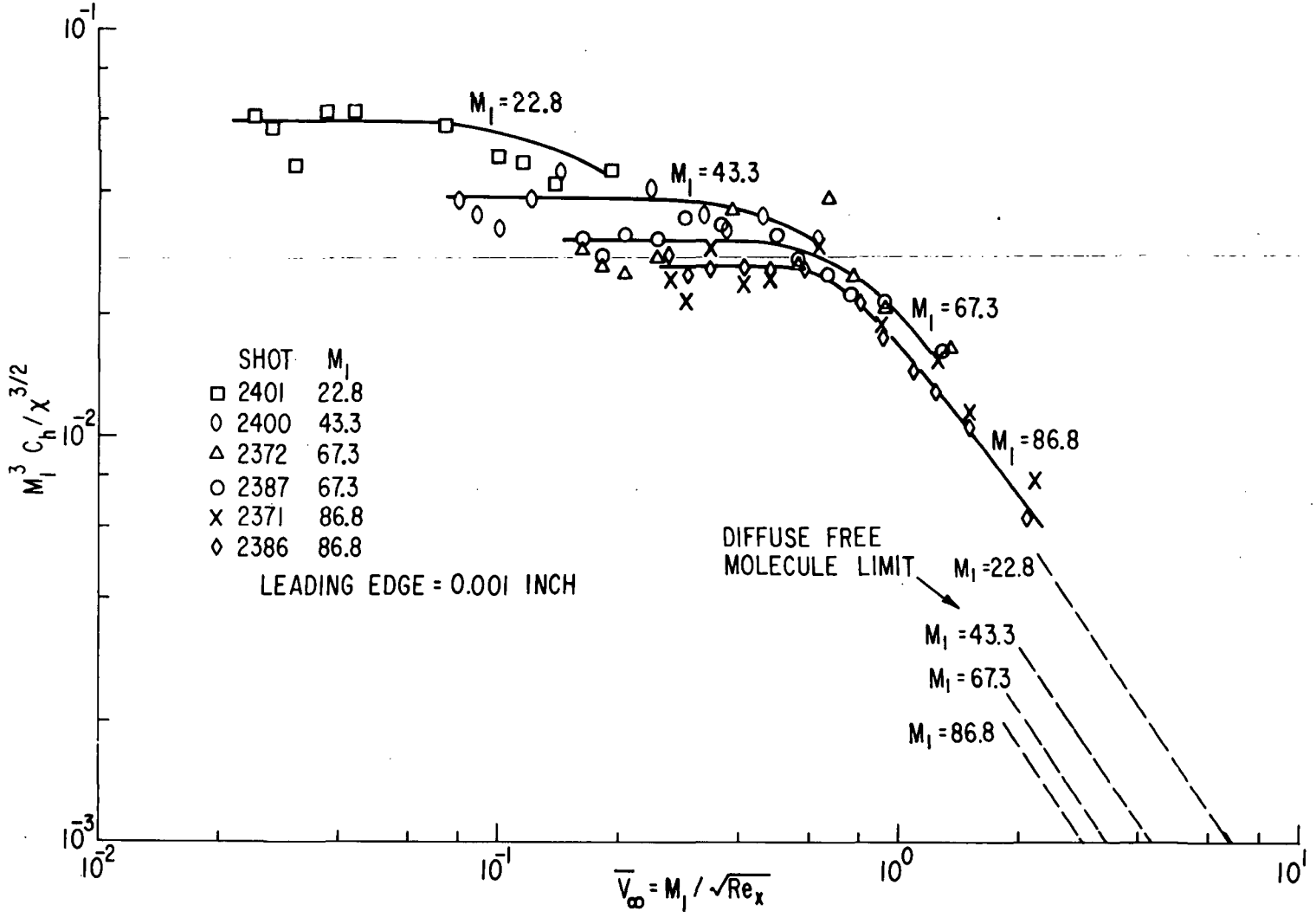

FIG.5 NORMALIZED HEAT TRANSFER COEFFICIENT AS FUNCTION OF RAREFACTION PARAMETER WITH HELIUM, M_1 =22.8 TO 86.8

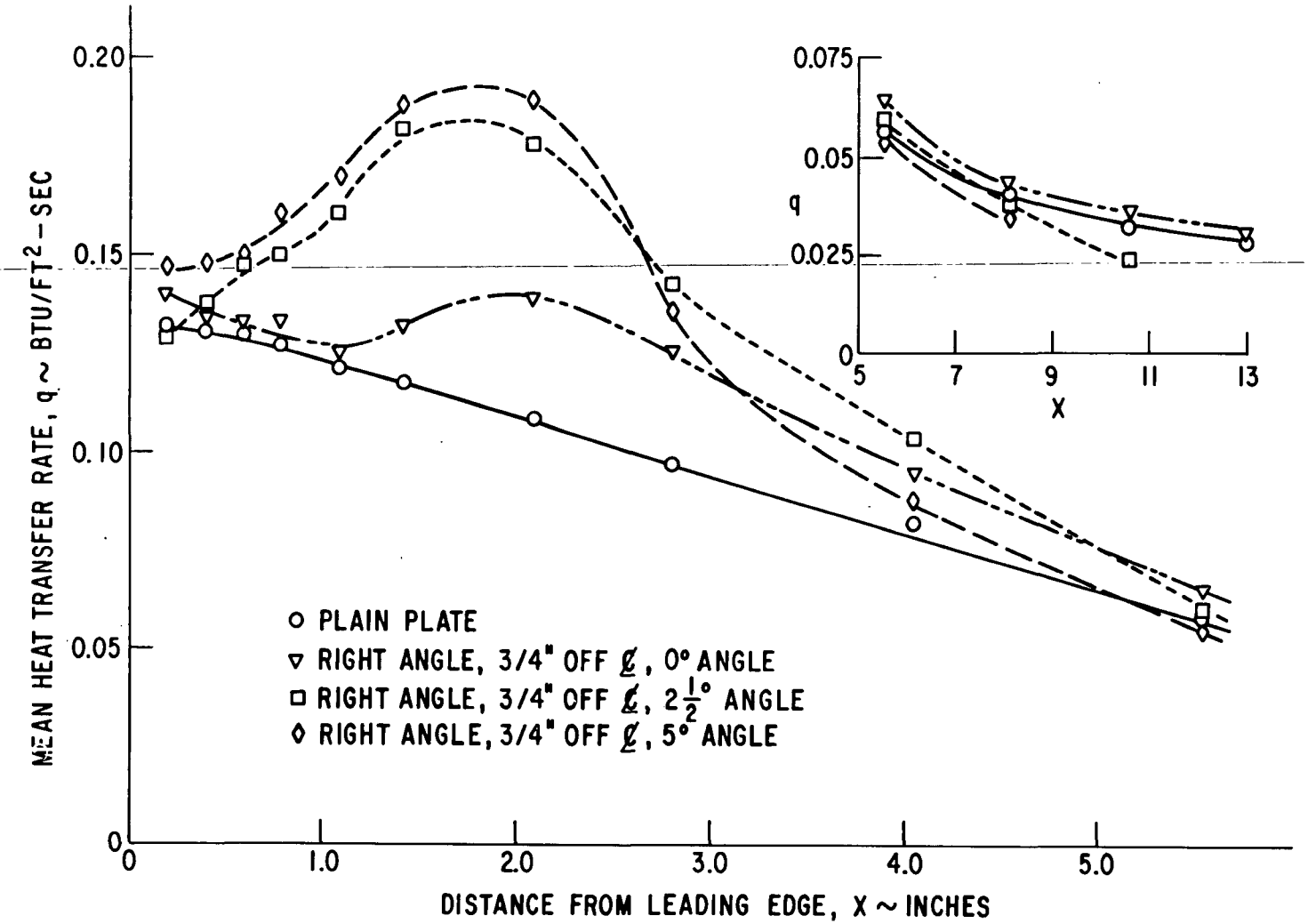

FIG.6a HEAT TRANSFER DISTRIBUTION ALONG HORIZONTAL PLATE WITH VERTICAL PLATE AT DIFFERENT ANGLE OF ATTACK, $P_5 \sim 80$ PSIA, $T_5 \sim 2385°R$, $Re/IN \sim 1035$, $M_1 = 19.0$

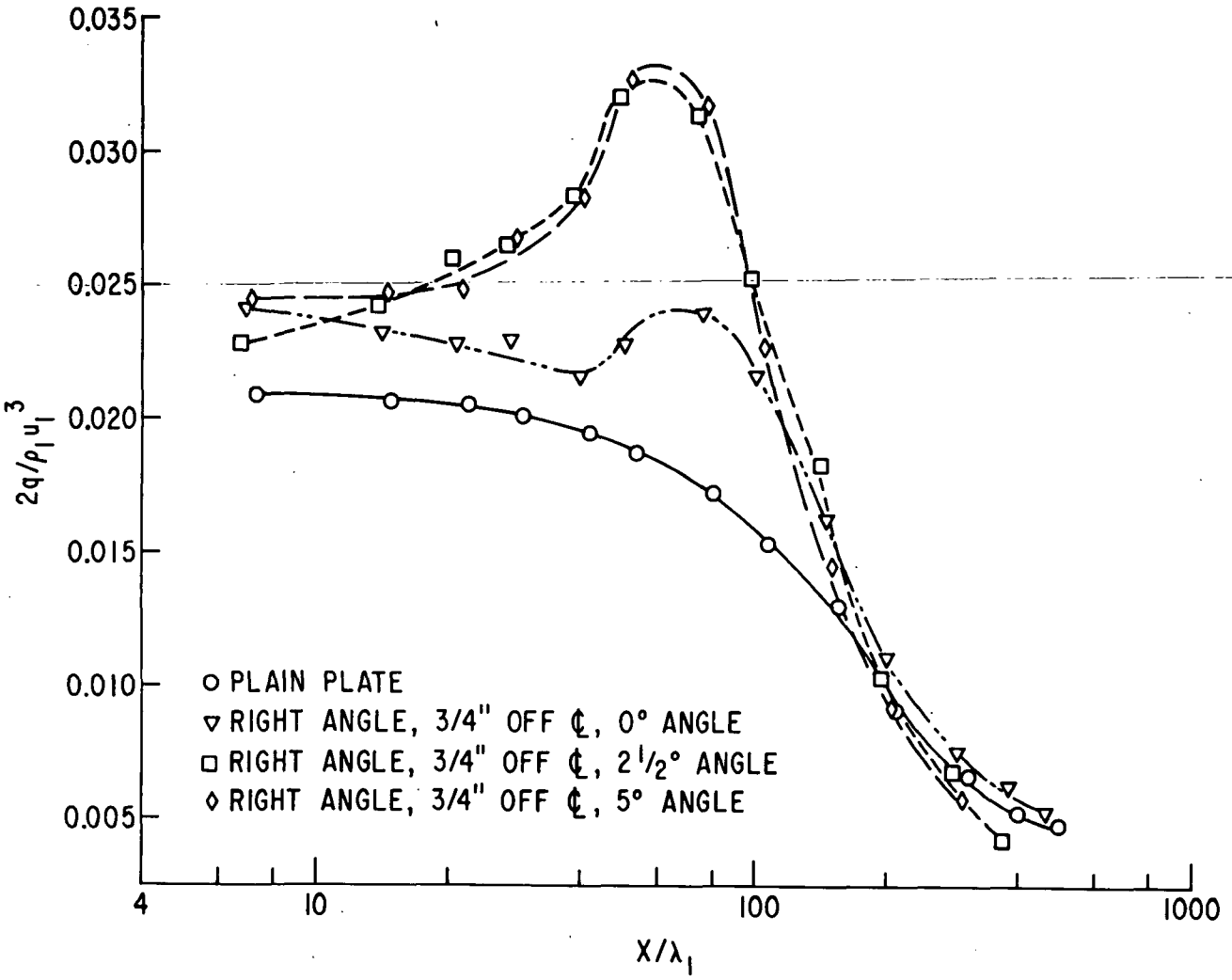

FIG.6b NORMALIZED HEAT TRANSFER RATE vs DISTANCE ALONG PLATE IN MEAN FREE PATHS, P_5~80 PSIA, T_5~2385°R, Re/IN~1035, M_1=19.0

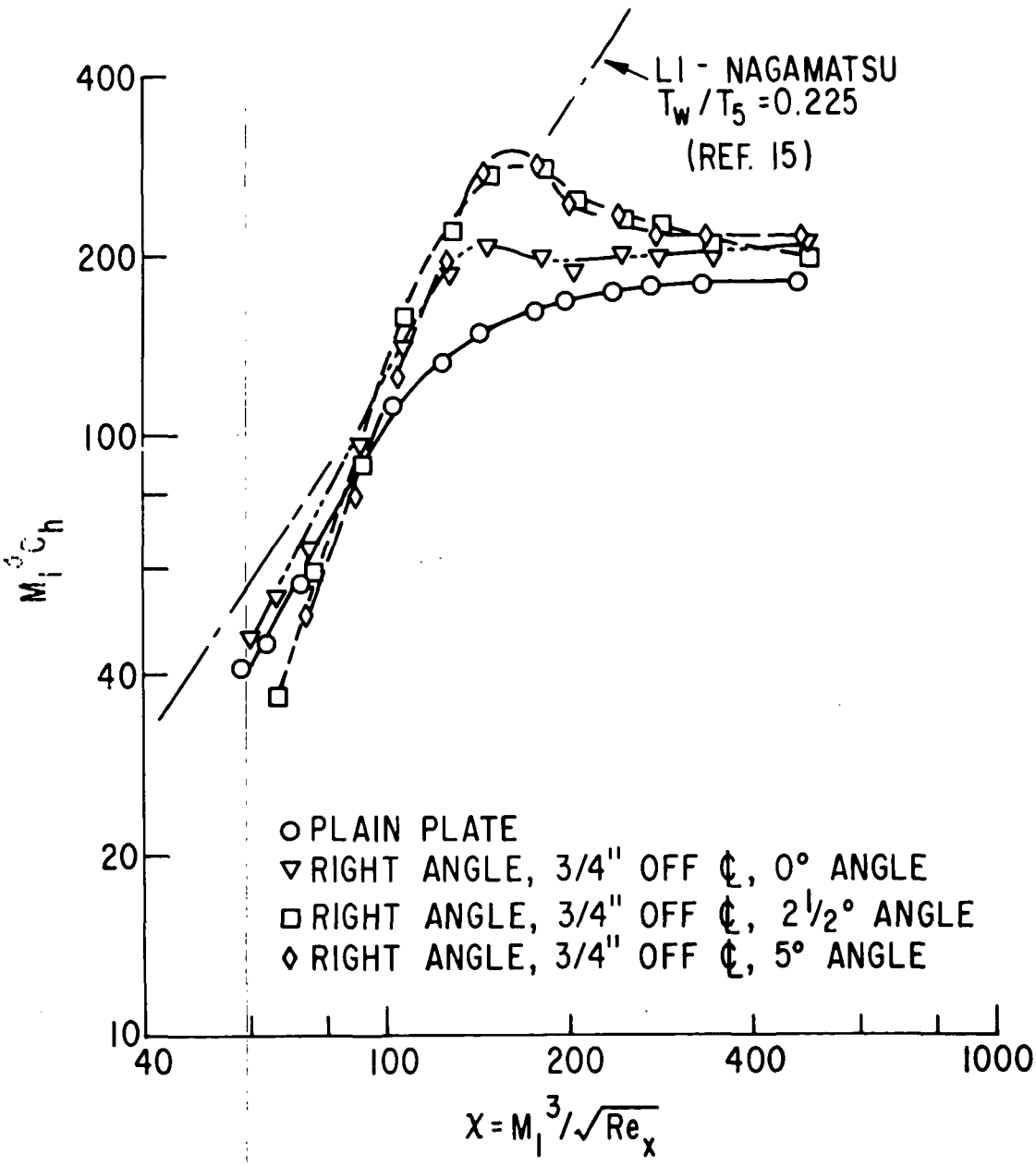

FIG.6c HEAT TRANSFER COEFFICIENT AS A FUNCTION OF STRONG INTERACTION PARAMETER, $P_5 \sim 80$ PSIA, $T_5 \sim 2385°R$, $Re/IN \sim 1035$, $M_1 = 19.0$

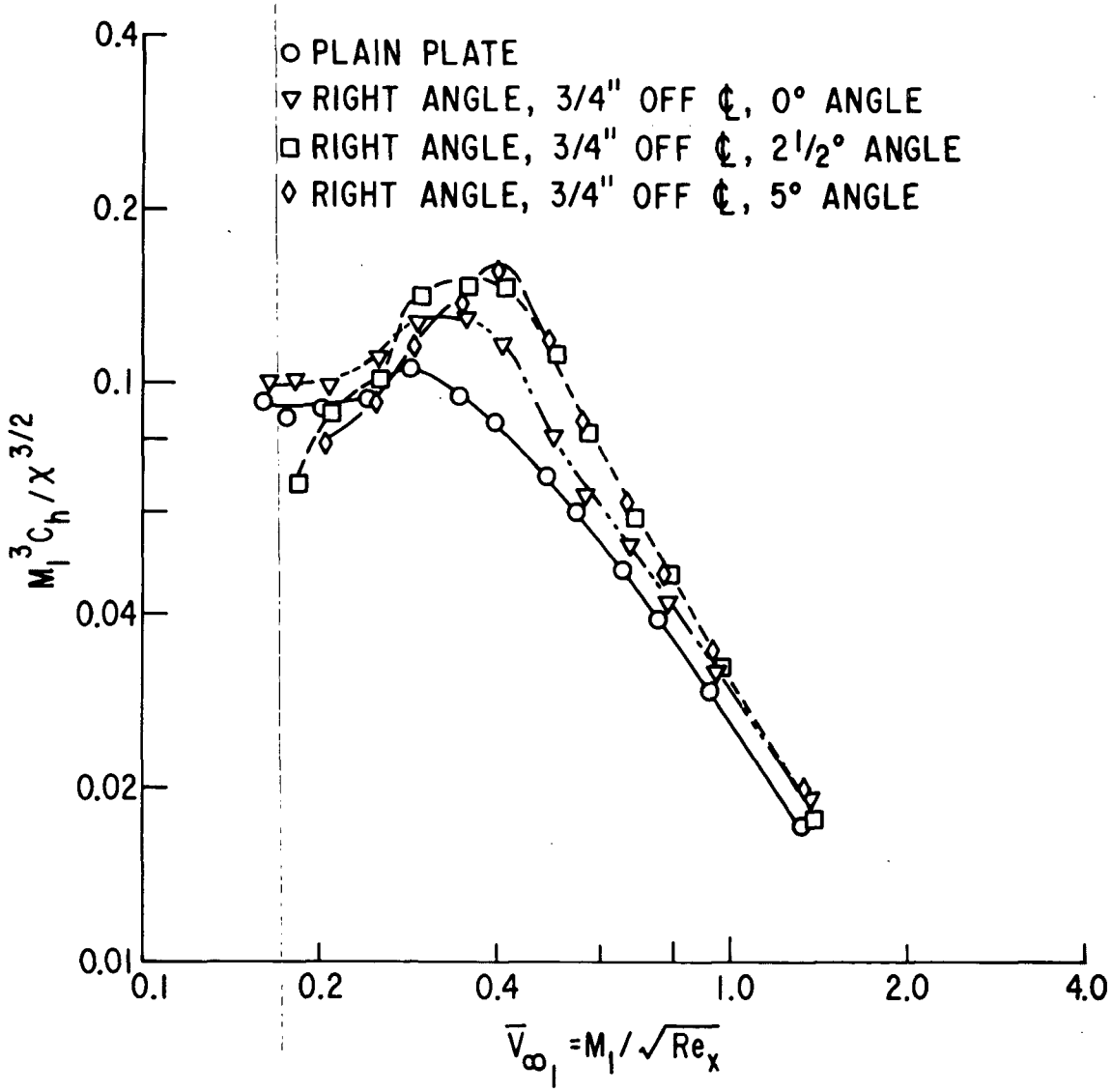

FIG.6d NORMALIZED HEAT TRANSFER COEFFICIENT AS A FUNCTION OF RAREFACTION PARAMETER, $P_5 \sim 80$ PSIA, $T_5 \sim 2385°R$, Re/IN~1035, $M_1 = 19.0$

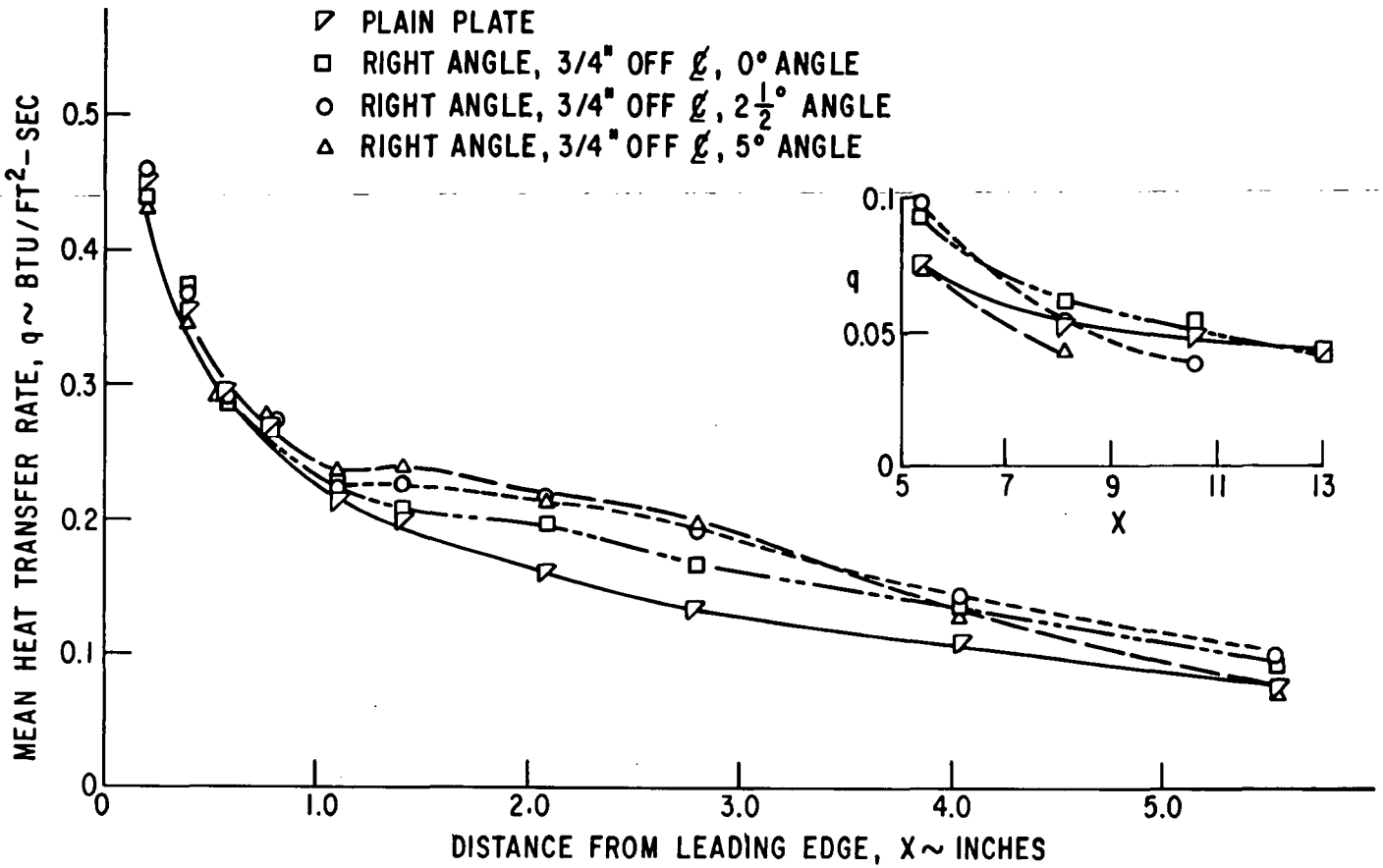

FIG.7a HEAT TRANSFER DISTRIBUTION ALONG HORIZONTAL PLATE WITH VERTICAL PLATE AT DIFFERENT ANGLE OF ATTACK, $P_5 \sim 296$ PSIA, $T_5 \sim 2295°R$, $Re/IN \sim 3950$, $M_1 = 19.1$

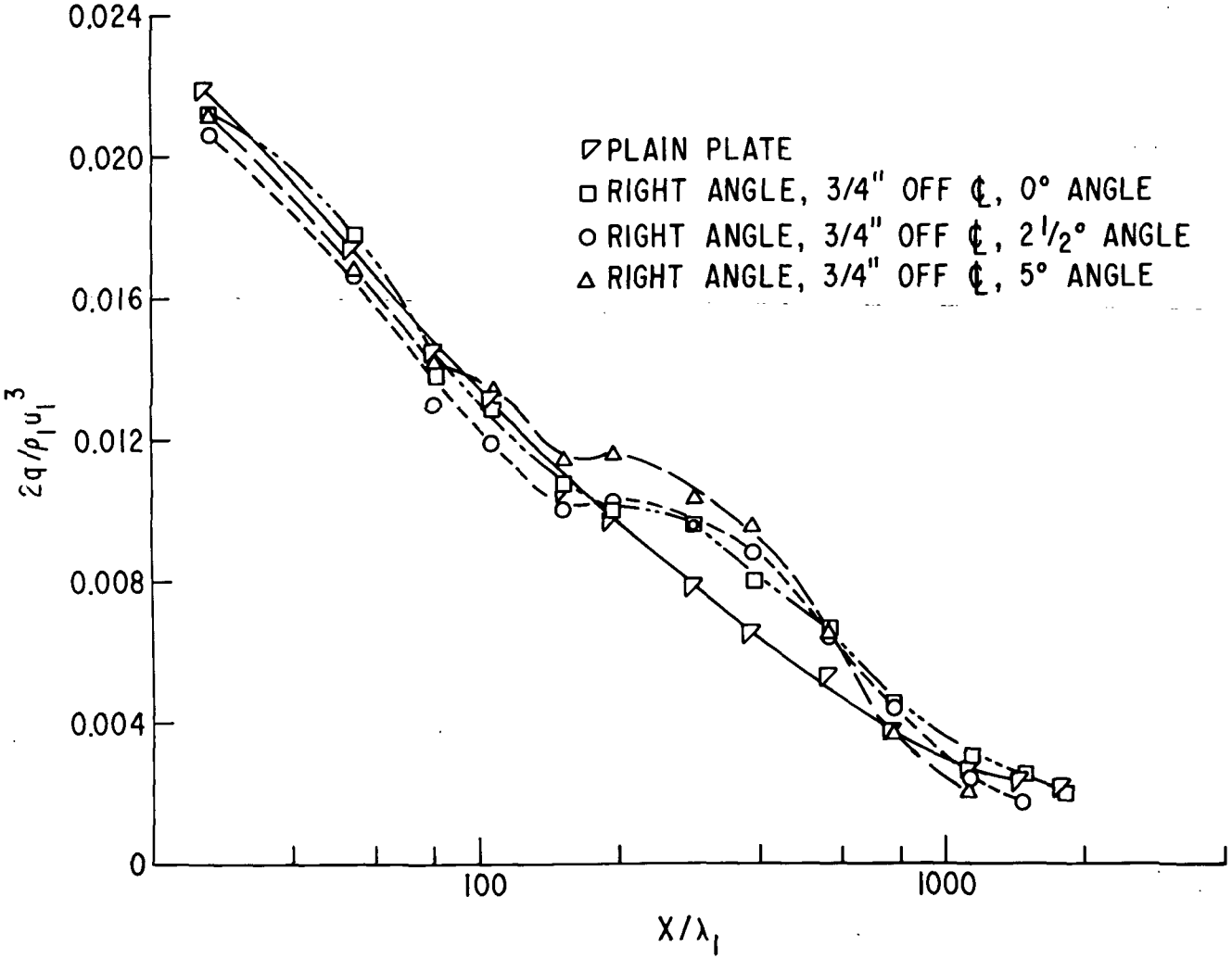

FIG. 7b NORMALIZED HEAT TRANSFER RATE vs DISTANCE ALONG PLATE IN MEAN FREE PATHS, $P_5 \sim 296$ PSIA, $T_5 \sim 2295°R$, $Re/IN \sim 3950$, $M_1 = 19.1$

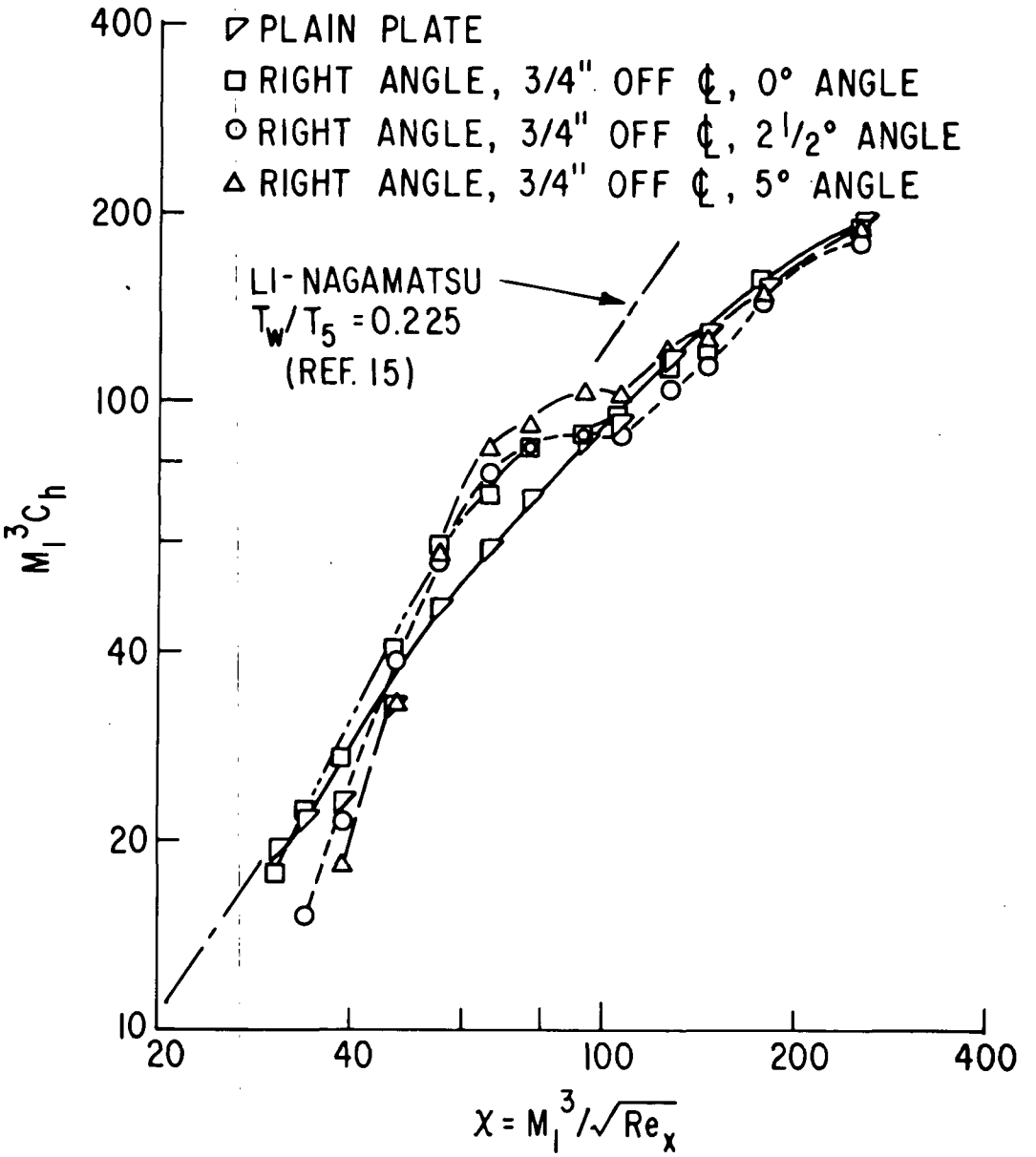

FIG.7c HEAT TRANSFER COEFFICIENT AS A FUNCTION OF STRONG INTERACTION PARAMETER, P_5~296 PSIA, T_5~2295°R, Re/IN~3950, M_1=19.1

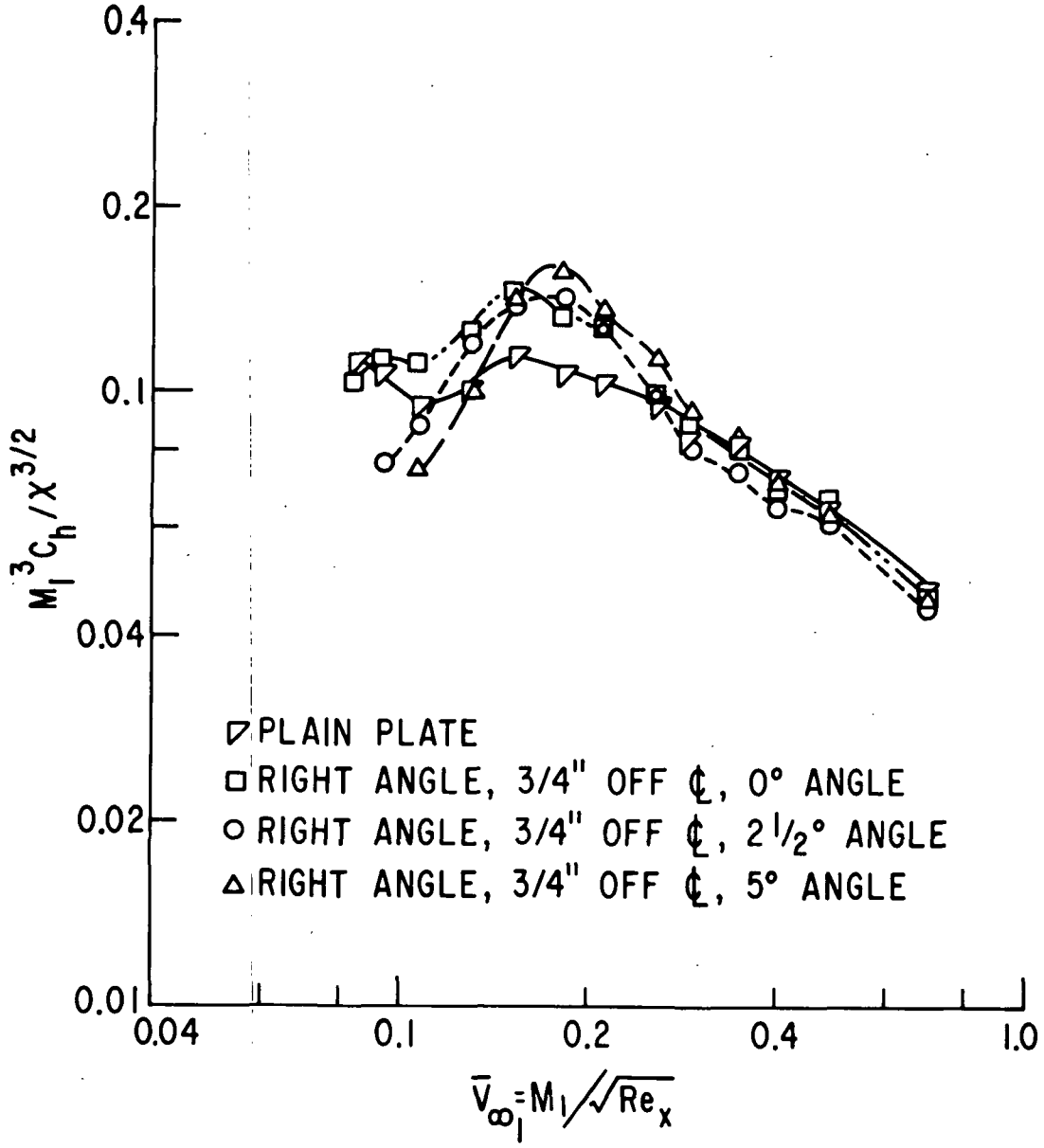

FIG. 7d NORMALIZED HEAT TRANSFER COEFFICIENT AS FUNCTION OF RAREFACTION PARAMETER, $P_5 \sim 296$ PSIA, $T_5 \sim 2295°R$, $Re/IN \sim 3950$, $M_1 = 19.1$

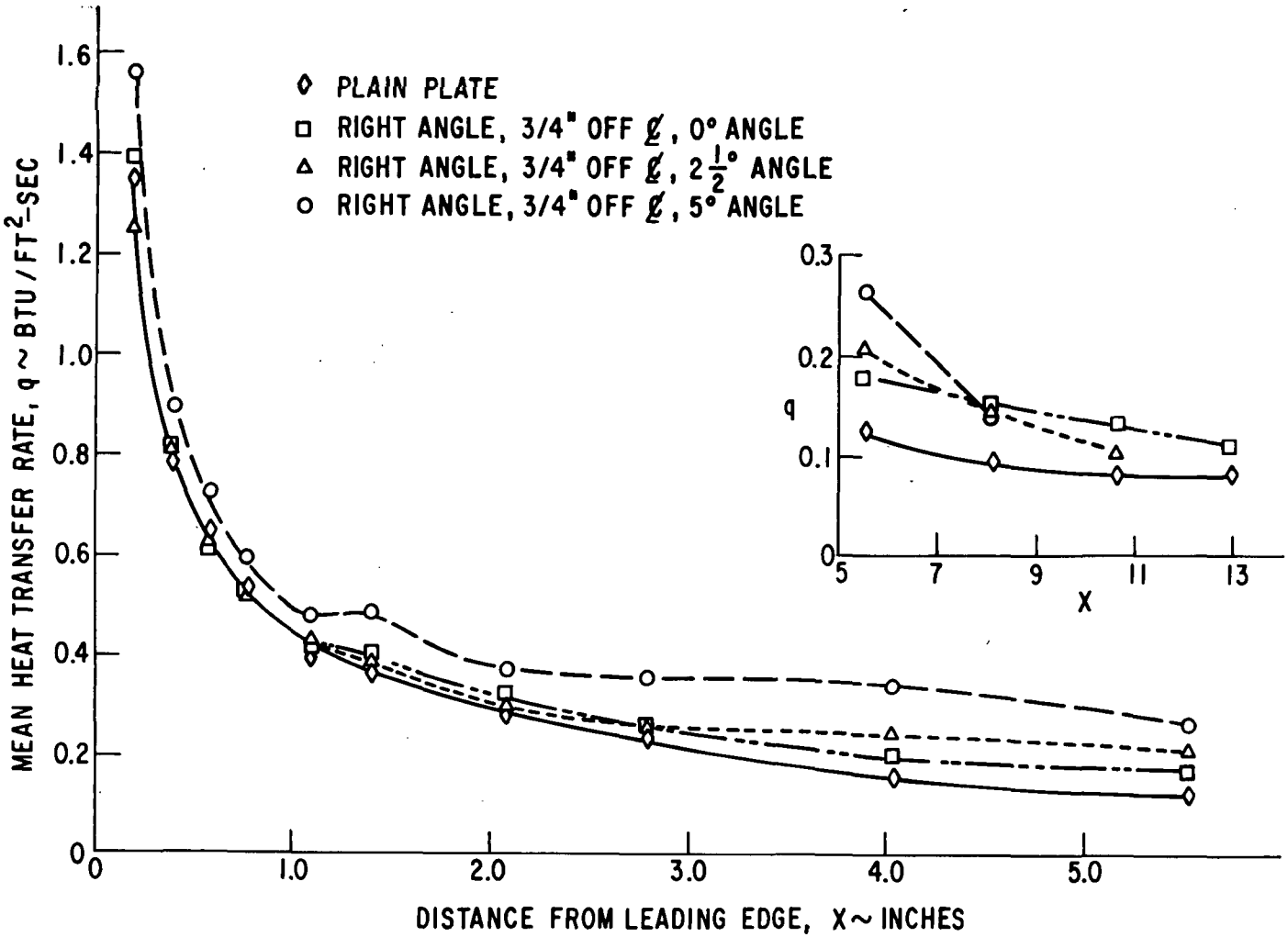

FIG.8a HEAT TRANSFER DISTRIBUTION ALONG HORIZONTAL PLATE WITH VERTICAL PLATE AT DIFFERENT ANGLE OF ATTACK, $P_5 \sim 1320$ PSIA, $T_5 \sim 2340°R$, $Re/IN \sim 17,330$, $M_1 = 19.1$

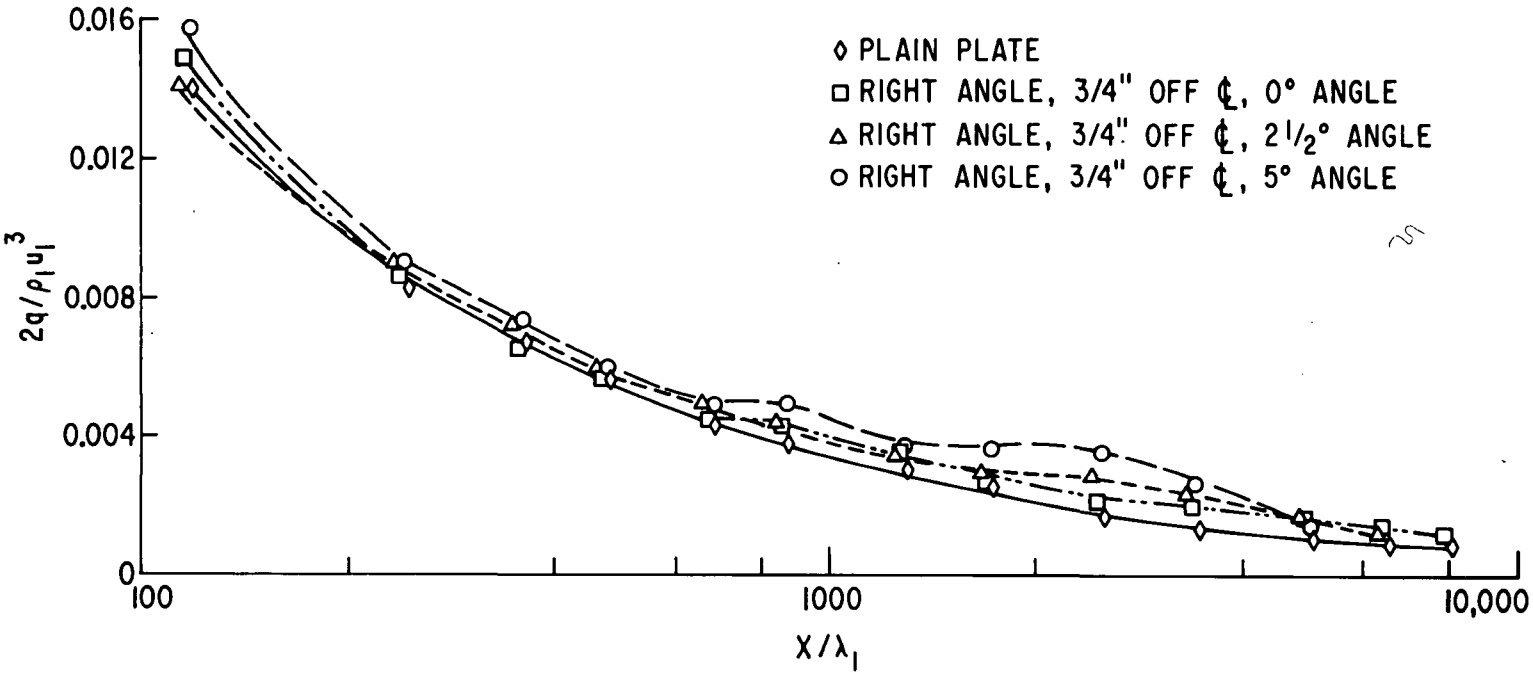

FIG.8b NORMALIZED HEAT TRANSFER RATE vs DISTANCE ALONG PLATE IN MEAN FREE PATHS, $P_5 \sim 1320$ PSIA, $T_5 \sim 2340°R$, $Re/IN \sim 17{,}330$, $M_1 = 19.1$

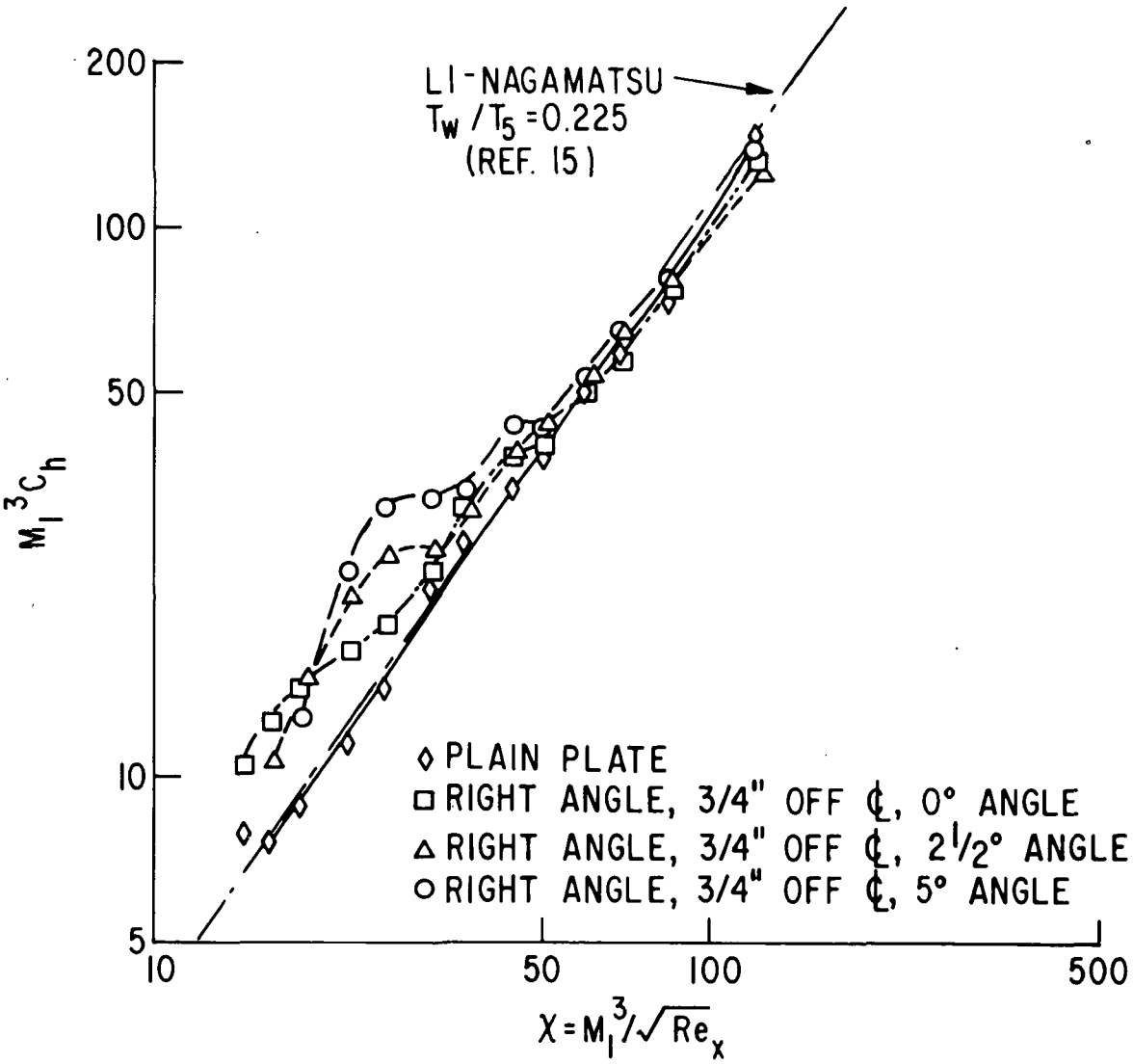

FIG.8c HEAT TRANSFER COEFFICIENT AS A FUNCTION OF STRONG INTERACTION PARAMETER, $P_5 \sim 1320$ PSIA, $T_5 \sim 2340°R$, $Re/IN \sim 17{,}330$, $M_1 = 19.1$

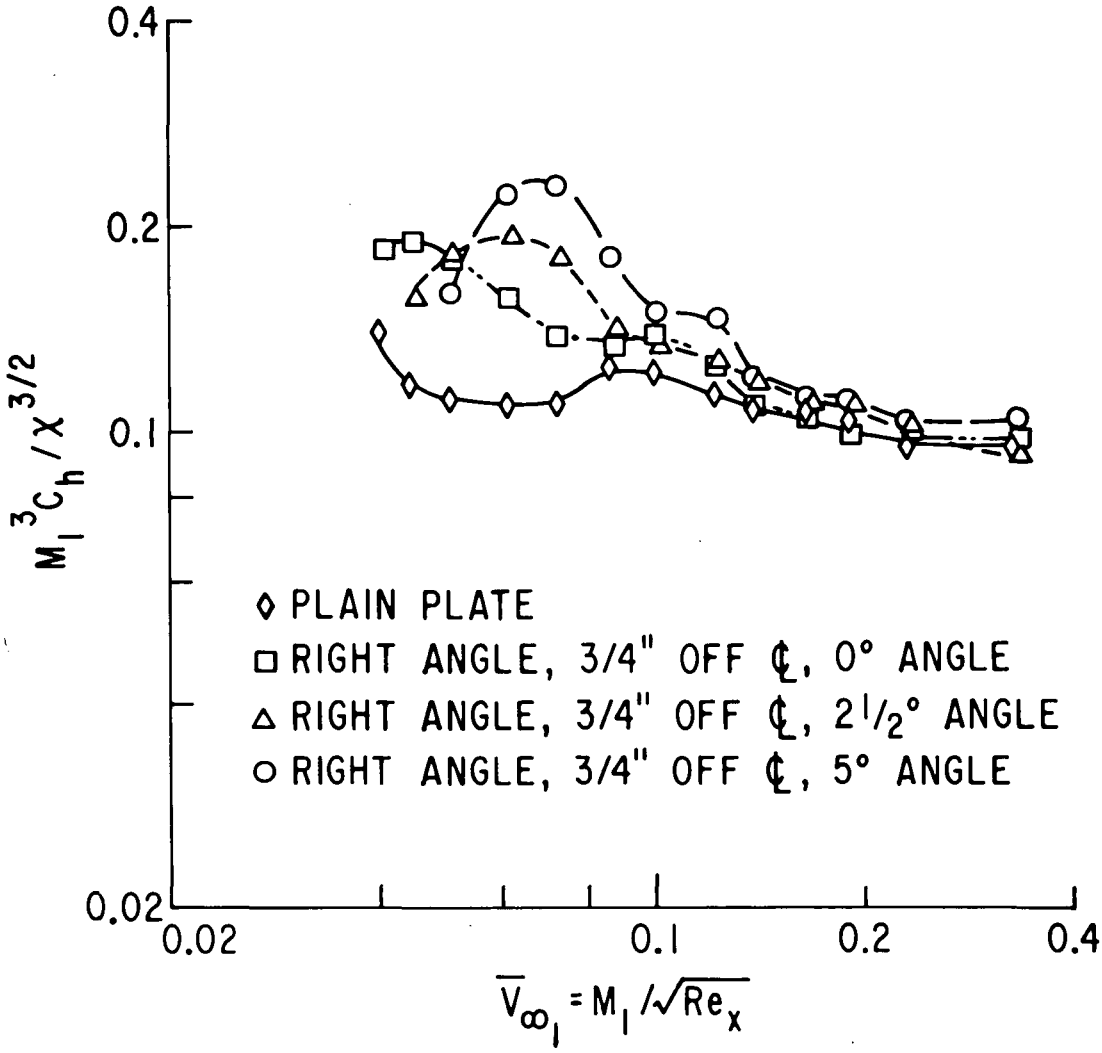

FIG.8d NORMALIZED HEAT TRANSFER COEFFICIENT AS FUNCTION OF RAREFACTION PARAMETER, $P_5 \sim 1320$ PSIA, $T_5 \sim 2340°R$, Re/IN~17,330, $M_1 = 19.1$